A new metriacanthosaurid theropod dinosaur from the Middle Jurassic of Yunnan Province, China (#106452)

First submission

Guidance from your Editor

Please submit by **11 Oct 2024** for the benefit of the authors (and your token reward) .

Structure and Criteria
Please read the 'Structure and Criteria' page for guidance.

Custom checks
Make sure you include the custom checks shown below, in your review.

Author notes
Have you read the author notes on the guidance page?

Raw data check
Review the raw data.

Image check
Check that figures and images have not been inappropriately manipulated.

If this article is published your review will be made public. You can choose whether to sign your review. If uploading a PDF please remove any identifiable information (if you want to remain anonymous).

Files

Download and review all files from the materials page.

15 Figure file(s)
3 Other file(s)

Custom checks

New species checks

- Have you checked our new species policies?
- Do you agree that it is a new species?
- Is it correctly described e.g. meets ICZN standard?

Structure and Criteria

Structure your review

The review form is divided into 5 sections. Please consider these when composing your review:

1. **BASIC REPORTING**
2. **EXPERIMENTAL DESIGN**
3. **VALIDITY OF THE FINDINGS**
4. General comments
5. Confidential notes to the editor

You can also annotate this PDF and upload it as part of your review

When ready submit online.

Editorial Criteria

Use these criteria points to structure your review. The full detailed editorial criteria is on your guidance page.

BASIC REPORTING

- Clear, unambiguous, professional English language used throughout.
- Intro & background to show context. Literature well referenced & relevant.
- Structure conforms to PeerJ standards, discipline norm, or improved for clarity.
- Figures are relevant, high quality, well labelled & described.
- Raw data supplied (see PeerJ policy).

EXPERIMENTAL DESIGN

- Original primary research within Scope of the journal.
- Research question well defined, relevant & meaningful. It is stated how the research fills an identified knowledge gap.
- Rigorous investigation performed to a high technical & ethical standard.
- Methods described with sufficient detail & information to replicate.

VALIDITY OF THE FINDINGS

- **Impact and novelty is not assessed.** Meaningful replication encouraged where rationale & benefit to literature is clearly stated.
- All underlying data have been provided; they are robust, statistically sound, & controlled.
- Conclusions are well stated, linked to original research question & limited to supporting results.

Standout reviewing tips

The best reviewers use these techniques

Tip	*Example*
Support criticisms with evidence from the text or from other sources	*Smith et al (J of Methodology, 2005, V3, pp 123) have shown that the analysis you use in Lines 241-250 is not the most appropriate for this situation. Please explain why you used this method.*
Give specific suggestions on how to improve the manuscript	*Your introduction needs more detail. I suggest that you improve the description at lines 57- 86 to provide more justification for your study (specifically, you should expand upon the knowledge gap being filled).*
Comment on language and grammar issues	*The English language should be improved to ensure that an international audience can clearly understand your text. Some examples where the language could be improved include lines 23, 77, 121, 128 – the current phrasing makes comprehension difficult. I suggest you have a colleague who is proficient in English and familiar with the subject matter review your manuscript, or contact a professional editing service.*
Organize by importance of the issues, and number your points	*1. Your most important issue* *2. The next most important item* *3. …* *4. The least important points*
Please provide constructive criticism, and avoid personal opinions	*I thank you for providing the raw data, however your supplemental files need more descriptive metadata identifiers to be useful to future readers. Although your results are compelling, the data analysis should be improved in the following ways: AA, BB, CC*
Comment on strengths (as well as weaknesses) of the manuscript	*I commend the authors for their extensive data set, compiled over many years of detailed fieldwork. In addition, the manuscript is clearly written in professional, unambiguous language. If there is a weakness, it is in the statistical analysis (as I have noted above) which should be improved upon before Acceptance.*

A new metriacanthosaurid theropod dinosaur from the Middle Jurassic of Yunnan Province, China

Yi Zou [1, 2], **Li Chen** [3], **Tao Wang** [4], **Guo-Fu Wang** [3], **Wei-Gang Zhang** [5], **Xiao-Qin Zhang** [6], **Zhen-Ji Wang** [6], **Xiao-Chun Wu** [7], **Hai-Lu You** [Corresp. 1, 2]

[1] Key Laboratory of Vertebrate Evolution and Human Origins, Institute of Vertebrate Paleontology and Paleoanthropology, Chinese Academy of Sciences, Beijing, China

[2] College of Earth and Planetary Sciences, Institute of Vertebrate Paleontology and Paleoanthropology, Chinese Academy of Sciences, Beijing, China

[3] Chuxiong Prefectural Museum, Chuxiong, China

[4] Center for Dinosaur Research and Protection, Bureau of Natural Resources of Lufeng City, Lufeng, China

[5] Chuxiong Jurassic Cultural Tourism Industrial Park Development Co. Ltd, Chuxiong, China

[6] Chuxiong Normal University, Chuxiong, China

[7] Canadian Museum of Nature, Ottawa, Canada

Corresponding Author: Hai-Lu You
Email address: youhailu@ivpp.ac.cn

Metriacanthosaurid theropods represent a basal-branching lineage of tetanurans. Members of this clade are mainly medium to large-sized and lived in Laurasia during the Middle Jurassic to the Early Cretaceous. In this clade, *Sinraptor dongi*, *Sinraptor hepingensis*, and *Yangchuanosarus shangyouensis* from the Late Jurassic are well represented by the nearly complete specimens, but the incompleteness of Middle Jurassic taxa hinders our knowledge of the origin and early evolution of Metriacanthosauridae. This paper describes a new genus and species of metriacanthosaurids, *Yuanmouraptor jinshajiangensis* gen. et sp. nov, from the Middle Jurassic Zhanghe Formation of Yunnan Province, China. The new taxon is represented by a cranium and the anterior section of the vertebral column including the complete cervical series and the first dorsal vertebra. *Yuanmouraptor jinshajiangensis* can be diagnosed based on the following autapomorphies: the anterior process of postorbital is sheet-shaped and keeps consistent depth; gently sigmoidal ventral ramus of postorbital with a laterally twisted trough running along it; processes on the anterodorsal margin of the third and fourth cervical neural spines; strongly posteriorly elongated epipophyses of anterior cervical vertebrae; deeply excavated pleuroceols on the third cervical vertebra; sheet-shaped and subrectangular neural spines of posterior cervical vertebrae. Phylogenetic analysis recovers *Yuanmouraptor* as the most basal-branching member within Metriacanthosauridae and provides a new alternative phylogenetic topology of non-coelurosaurian tetanurans.

A new metriacanthosaurid theropod dinosaur from the Middle Jurassic of Yunnan Province, China

Yi Zou[1,2], Li Chen[3], Tao Wang[4], Guo-Fu Wang[3], Wei-Gang Zhang[5], Xiao-Qin Zhang[6], Zhen-Ji Wang[6], Xiao-Chun Wu[7], Hai-Lu You[1,2]

[1] Key Laboratory of Vertebrate Evolution and Human Origins, Institute of Vertebrate Paleontology and Paleoanthropology, Chinese Academy of Sciences, Beijing, China
[2] College of Earth and Planetary Sciences, University of Chinese Academy of Sciences, Beijing, China
[3] Chuxiong Prefectural Museum, Chuxiong, China
[4] Center for Dinosaur Research and Protection, Bureau of Natural Resources of Lufeng City, Lufeng, China
[5] Chuxiong Jurassic Cultural Tourism Industrial Park Development Co. Ltd., Chuxiong, China
[6] Chuxiong Normal University, Chuxiong, China
[7] Canadian Museum of Nature, Ottawa, Canada

Corresponding Author:
Hai-Lu You[1]

Email address: youhailu@ivpp.ac.cn

INTRODUCTION

Metriacanthosauridae is a family of medium-to-large sized carnivorous dinosaurs and represents a basal-branching clade within the Allosauroidea (*Holtz et al., 2004; Smith et al., 2007; Benson, 2010; Carrano et al., 2012; Hendrickx et al., 2015; Coria & Currie, 2016; Rauhut et al., 2016, 2019, 2024; Lamanna et al., 2020*). Members of this clade mainly came from the Middle to Late Jurassic strata of western China (Fig. 1), such as Sichuan, Chongqing, Xinjiang, and Yunnan (*Dong et al., 1978, 1983; Gao, 1992, 1993, 1999; Currie & Zhao, 1993; Wu et al., 2009*). Apart from these taxa found in China, metriacanthosaurid theropods were also reported in the Late Jurassic of England (Huene, 1923; Walker, 1964), the Late Jurassic of Kyrgyzstan (*Rauhut et al., 2024*), and the Early Cretaceous of Thailand (*Buffetaut et al., 1996*). Recently, *Yu et al. (2023)* reported the probable distribution of this clade in the Tibetan Plateau.

Here we report a new genus and species of Metriacanthosauridae collected from the Middle Jurassic Zhanghe Formation of Jiangyi, Yuanmou county of Yunnan Province, China (Fig.1 B). Material of this new taxon include a relatively complete skull and the first 11 vertebrae including 10 cervical vertebrae and the anterior-most dorsal vertebra. The Zhanghe Formation also yielded sauropods including *Yuanmousaurus* (*Lü et al., 2006*), *Eomamenchisaurus* (*Lü et al., 2008*), and *Nebulasaurus* (*Xing et al., 2015*). Our phylogenetic analysis suggests that the new taxon is probably one of the two most basal-branching metriacanthosaurids. Furthermore, some characters present in the new taxon are also shared with several megalosauroids (*Li et al., 2009; Dai et al., 2020*) and non-tetanuran theropods (*Colbert, 1989; Marsh & Rowe, 2020*), which suggests that these shared characters were gained independently by the aforementioned taxa.

MATERIAL & MATHODS

Material

The specimens studied here were excavated by a field team of Chuxiong Prefectural Museum from a layer of red sandstones within the Zhanghe Formation at Jiangyi Town, Yuanmou County, Chuxiong Yi Autonomous Prefecture, Yunnan, China in 2006, and is now on display in the museum of Lufeng World Dinosaur Valley in Lufeng City, Yunnan Province. Most cranial bones are still in articulation or closely associated. Some of the cranial elements are heavily distorted or covered by matrix or other bones, rendering difficult or impossible to determine bone sutures or internal structures. The specimen was prepared using mechanical tools (pneumatic chisels) and photographed from various perspectives with a Sony DLSR-A700 digital camera. Line drawings were made based on the reference photographs and checked against the original specimens.

Phylogenetic analysis

The new matrix for the phylogenetic analysis in this study was modified based on that of *Carrano et al. (2012)*, which mainly focused on the phylogenetic relationship within tetanurans. We added five new and 26 characters modified from the datasets of *Lamanna et al. (2020)*, *Eddy & Clark (2011)*, *Brusatte & Serreno (2008)*, and *Schade et al. (2023)* (see the online Supplemental File S1 for details). We added the coelophysoid *Panguraptor* (*You et al., 2014*), *Zuolong* (*Choiniere et al., 2010*), *Guanlong* (*Xu et al., 2006*), and *Eoabelisaurus* (*Pol & Rauhut, 2012*) to the matrix to enrich the samples of non-tetanurans, Coelurosauria, and Ceratosauria, respectively. Several basal-branching tetanurans such as *Asfaltovenator* (*Rauhut & Pol, 2019*), *Wiehenvenator* (*Rauhut et al., 2016*), and *Yunyangosaurus* (*Dai et al., 2020*) were added because these taxa were recently reported tetanurans. *Alpkarakush kyrgyzicus* (*Rauhut et al., 2024*) (the most recently named Central Asian metriacanthosaurid) was also added to the dataset. The new matrix, consisting of 372 characters and 70 operational taxonomic units (OTUs), was analyzed using TNT v. 1.6 (*Goloboff & Catalano, 2023*). The most parsimonious trees (MPTs) were recovered by a traditional search of 1000 replicates of Wagner trees followed by tree bisection and reconnection, with 10 trees saved per replication. Characters were equally weighted, and none of the characters were treated as ordered.

Nomenclatural acts

The electronic version of this article in Portable Document Format (PDF) will represent a published work according to the International Commission on Zoological Nomenclature (ICZN), and hence the new names contained in the electronic version are effectively published under that Code from the electronic edition alone. This published work and the nomenclatural acts it contains have been registered in ZooBank, the online registration system for the ICZN. The ZooBank LSIDs (Life Science Identifiers) can be resolved and the associated information viewed through any standard web browser by appending the LSID to the prefix http://zoobank.org/. The LSID for this publication is: urn:lsid:zoobank.org:pub:2A9F32AD-B671-4F48-8A6E-0A69976A75FB. The online version of this work is archived and available from the following digital repositories: PeerJ, PubMed Central SCIE and CLOCKSS.

RESULTS

Systematic paleontology

Dinosauria *Owen, 1842*

Theropoda *Marsh, 1881*

Tetanurae *Gauthier, 1986*

Allosauroidea Currie & Zhao, 1993

Metriacanthosauridae Paul, 1988

Yuanmouraptor gen. nov.

Diagnosis—As for the only species.

Yuanmouraptor jinshajiangensis gen. et sp. nov.

Etymology—The genus name, '*Yuanmou'*, refers to Yuanmou County where the holotype was collected, and 'raptor' is Latin for the robber. The specific name, '*jinshajiang'* (the middle region of Yangtze River) which passes through Yuanmou County and the type locality is located on the north bank of the river.

Holotype—LFGT-ZLJ0115: a partial skeleton consists of a nearly complete skull with mandible and 11 articulated anterior vertebrae including 10 cervical vertebrae and the first dorsal vertebra.

Type Locality and horizon—Jiangyi Town, Yuanmou County, Chuxiong Yi Autonomous Prefecture, Yunnan Province, China; Zhanghe Formation, early Middle Jurassic, Aalenian/Bajocian ((Bureau of Geology and Mineral Resources of Yunnan Province 1990).

Diagnosis—A medium-sized metriacanthosaurid dinosaur differing from other metriacanthosaurids by the following unique combination of characters (autapomorphies are indicated with an asterisk): ventral extension of antorbital fossa on maxilla is dorsoventrally deep, which is shared with non-tetanurans, *Marshosaurus* and *Eocarcharia*, and some basal-branching coelurosaurs such as *Ornitholestes* and *Proceratosaurus*; an accessory foramen located within antorbital fossa on lacrimal and ventral to pneumatic foramen, similar to *Allosaurus*; dorsal part of postorbital forming a very low rugosity, similar to megalosaurids ; lack of pneumatic fenestra on lateral surface of jugal, shared with non-tetanurans; the anterior process of postorbital sheet-shaped and its depth keeping consistent*; gently sigmoidal ventral ramus of postorbital with a laterally twisted trough running along it*; process on anterodorsal margin of the third and fourth cervical vertebrae*; flattened peripheral band on anterior articular surface of anterior cervical centra, shared with *Yunyangosaurus* and megalosaurids; strongly posteriorly elongated epipophyses on anterior cervical vertebrae*; deeply excavated pleuroceols on the third cervical vertebra*; sheet-shaped and subrectangular neural spines of posterior cervical vertebrae*.

General description of the cranium

The conditions of preservation of LFGT-ZLJ0115 are different between each side, and bones show many fractures which might be caused during fluvial transportation. On the left side (Fig. 2 A B), most parts of the nasal and elements around the orbit and lateral temporal fenestra are missing. On the right side (Fig. 2 C D), although the nasal is also poorly preserved, other bones are relatively more complete than those of the left side. The mandibular ramus is well-preserved on both sides. The remnant elements of the skull and mandible are generally articulated, and thus most of the internal structures are obscured from observation except the right ramus of the mandible. The main fenestrae of the skull, such as the naris, antorbital fenestra, orbit, lateral temporal fenestra, and supratemporal fenestra, are all damaged or largely distorted. The preserved skull is measured 53.9 cm in anteroposterior length, and the reconstruction (Fig. 3) of the skull measures 60. 1 cm in anteroposterior length. In comparison, the type specimen of *Yangchuanosaurus shangyouensis (Dong et al., 1978*) bears a skull length of 78 cm, and the referred specimen (*Y. magnus*, reported by *Dong et al. [1983]*, was considered to present different ontogenetic stage of *Y. shangyouensis* by *Carrano et al. [2012]*) has an estimated skull length of 111 cm. The skull of *Sinraptor dongi* (*Currie & Zhao, 1993*) is 90 cm long and the skull of *S. hepingensis* (*Gao, 1992, 1999*) is 104 cm long.

Based on the closed neurocentral suture, *Yuanmouraptor* is probably a mature individual.

Premaxilla—Only the left premaxilla (Fig. 4 A, B) is preserved, with most supranarial process missing except for its risen base. In lateral view, the outline of the premaxillary body (below the external naris) is roughly quadrangular and slightly higher than long (5.65×5.42 cm), with the ventral border of the external naris is nearly paralleled with the premaxillary alveolar margin, which is similar to the condition of *Ceratosaurus* (*Madsen & Welles, 2000*), *Torvosaurus* (*Britt, 1991*), *Majungasaurus* (*Sampson & Witmer, 2007*), and many allosauroids, such as *Sinraptor* (*Currie & Zhao, 1993; Gao, 1999*), and *Acrocanthosaurus* (*Eddy & Clarke, 2011*), but in contrast to *Sinraptor* (*Currie & Zhao, 1993*), *Allosaurus* (*Britt, 1991*), *Neovenator* (*Brusatte et al., 2008*), *Dubreuillosaurus* (*Allain, 2002*), *Marshosaurus* (*Madsen, 1976b*), and *Monolophosaurus* (*Brusatte et al., 2010a*), in which the premaxilla is slightly longer than high. ~~The premaxilla is much longer than high (length/height > 2) in spinosaurids like *Suchomimus* (*Sereno et al., 1998*) and *Ceratosuchops* (Barker et al., 2021).~~ The premaxilla of *Yuanmouraptor* bears four alveoli, which is a primitive condition for theropods (*Allain, 2002*; *Sampson & Witmer, 2007*, *Currie & Zhao, 1993*), as in *Sinraptor*, *Yangchuanosaurus*, but five alveoli are present in *Allosaurus* and *Neovenator* (*Brusatte et al., 2008*). In spinosaurids, the number of alveoli could reach seven. The fourth tooth is broken with only a little part of its base preserved. The other three are complete and compress mediolaterally with slightly backward curvature. The distal carina is well-developed and extended throughout the whole length, whereas the mesial carina is only visible at the epical one third of the second tooth in lateral view (Fig. 4 C).

The anterodorsal border of the premaxillary body is missing, along with the main part of the supranarial process (nasal process), but the preserved base of the process forms the anteroventral margin of the external naris and indicates the posterodorsal orientation of the process. The narial fossa is located ventrally to the remnant part of the external naris as in *Acrocanthosaurus*, *Sinraptor*, *Allosaurus*, and *Dubreuillosaurus*. The complete portion of the anterodorsal rim suggests that the anterior margin of the premaxillary body is nearly vertical as in *Sinraptor*, *Ceratosaurus*, and *Allosaurus*, whereas that of *Torvosaurus*, *Dubreuillosaurus*, and *Duriavenator* (*Benson, 2008*) is more rounded and more posterodorsally inclined. The subnarial process (maxillary process) is relatively complete and of triangular-shape tapering posterodorsally in lateral view, resembling that of *Ceratosaurus*, *Neovenator*, and *Sinraptor* in relative size and orientation. The subnarial process in *Acrocanthosaurus* and *Allosaurus* is elongated dorsoposteriorly, whereas in *Duriavenator* this process is horizontally elongated without the dorsal inclination. The posteroventral rim of the subnarial process is confluent with the posterior border of the premaxillary body, and both form the slightly posterodorsally inclined suture with the maxilla in lateral view. The posterior border of the premaxillary body ventral to the subnarial process presents a rugose surface and indicates the overlying of the maxilla (Fig. 4 B). There is no evident subnarial foramen near the posterior border of the premaxillary body and subnarial process, whereas the subnarial foramen is well developed in *Allosaurus*, *Acrocanthosaurus*, *Sinraptor*, and other theropods. Based on the suture of the premaxilla with the maxilla, there is no subnarial gap between these two bones, and the tooth row of each bone is continuous and at the same level, as in most allosauroids.

Numerous foramina are mainly scattered on the lateral surface ventral to the mid height of the premaxillary body and open ventrolaterally, similar to the distribution pattern in *Sinraptor* and *Yangchuanosaurus*, whereas in many megalosaurids (*Dubreuillosaurus*, *Torvosaurus* and *Marshosaurus*) the foramina are mainly distributed on the anterior half of the premaxillary body. In *Neovenator*, the foramina spread evenly over the lateral surface of the premaxillary body. Recent research (*Carr et al., 2017; Barker et al, 2017; Cullen et al, 2023*) proposed that these foramina in terrestrial theropods probably house branches of trigeminal nerve linking to integumentary sensory organs, which are related to foraging, intraspecific communication and nest building behavior.

Maxilla—Both the left and right maxillae are adhered to the matrix, and thus the medial surface is obscured. The main body of the left maxilla (Fig. 4 E, F) is well-preserved but lacks most of its ascending ramus. The posterodorsally oriented base of the ascending ramus of the right maxilla (Fig. 4 G, H) is preserved, but the anterodorsal margin of the lateral surface is missing. The anteroposterior length of the preserved part of the left maxilla is measuring 28.87 cm, and the right element is 29 cm.

On the lateral surface, the ventral wall of the external antorbital fossa is very developed, occupying more than half of the maxillary body ventrally, as in *Masiakasaurus* (*Carrano et al., 2011*), *Marshosaurus* (*Madsen, 1976b*), and many allosauroids (*Currie & Zhao, 1993*; *Dong et al., 1983*; *Gao, 1999*; *Madsen, 1976a*, *Sereno & Brusatte, 2008*). This is different from the moderate range of the antorbital fossa wall reaching nearly half depth of the maxilla body in *Afrovenator* (*Serreno et al., 1994*), *Acrocanthosaurus* (*Eddy & Clark., 2011*), *Neovenator* (*Brusatte et al., 2008*), and *Ceratosaurus* (*Madsen & Welles, 2000*). In contrast, the antorbital fossa has very limited exposure on the maxillary body in *Torvosaurus* (*Britt, 1991*; *Hendrickx & Mateus, 2014*), *Wiehenvenator* (*Rauhut et al., 2016*), *Monolophosaurus* (*Zhao & Currie, 1993*; *Brusatte et al., 2010a*), and some Carcharodontosarurids (*Sereno et al., 1996*; *Coria & Salgado, 1995*; *Coria & Currie, 2006*; *Brusatte & Sereno, 2007*). Some abelisaurids even totally lack the antorbital fossa on the maxillary body like *Majungasaurus* (*Sampson & Witmer, 2007*) and *Kryptops* (*Sereno & Brusatte, 2008*). The border of the antorbital fossa is better preserved and well-defined by a rim on the left maxilla, while this rim is less developed on the right maxilla due to compression. The antorbital fossa is anteriorly extensive, whose anterior-most border reaches the 3rd alveolus, as in *Sinraptor* (*Currie & Zhao, 1993*) and *Ceratosaurus* (*Madsen & Welles, 2000*), indicating a reduced anterior ramus. Above the 3rd tooth the rim gently curves upward, forming a round anteroventral margin of the antorbital fossa as in *Sinraptor* (*Currie & Zhao, 1993*), *Yangchuanosaurus* (*Dong et al., 1983*), *Ceratosaurus* (*Madsen & Welles, 2000*), *Marshosaurus* (*Madsen, 1976b*), and *Monolophosaurus* (*Brusatte et al., 2010a*). This contrasts with the squared anteroventral border of the antorbital fossa in Eocarcharia (*Sereno & Brusatte, 2008*), *Acrocanthosaurus* (*Eddy & Clarke, 2011*), and *Dubreuillosaurus* (*Allain, 2002*). Posteriorly this rim flattens gradually throughout the length of the posterior ramus.

The preserved ascending ramus of the right maxilla preserves the anteroventral margin of the external antorbital fenestra. From the ventral margin of the antorbital fenestra, the preserved ascending ramus is measuring 6.95 cm. The angle between the main axis of the ascending ramus and the jugal ramus of the maxilla is not very sharp, and about 60°. The lateral surface of the ascending ramus of the right maxilla is too fragmentary to determine whether it is excavated by pneumatic openings (Fig. 4 G, H).

Although the ascending rami are heavily damaged on both maxillae, traces of two openings at the base of the ascending ramus are preserved. On the left maxilla, the anterior concavity on the anterodorsal margin of the maxillary body is smooth, demarcates the ventral rim of the promaxillary fenestra, and its anterior end is adjacent to the anteroventral margin of antorbital fossa. The posterior one only preserves its rounded ventral half. On the right maxilla, the anterior opening only preserves its posterior rim while the posterior one is nearly intact. These two openings are separately interpreted as promaxillary fenestra and maxillary fenestra here based on their relative placement (*Witmer, 1997*). The preserved portion of the promaxillary fenestra indicates that it is larger than the maxillary fenestra, which resembles the condition in *Sinraptor* (*Currie & Zhao, 1993*) and *Eocacharia* (*Sereno & Brusatte, 2008*). Relatively large promaxillary fenestra is regard as a synapomorphy of Metriacanthosauridae (Carrano et al., 2012), in many other theropod (*Allosaurus*, *Neovenator*, *Ceratosaurus*, *Dubreuillosaurus*: *Currie & Zhao, 1993*; *Brusatte et al., 2008*; *Madsen & Welles, 2000*; *Allain, 2002*) the promaxillary feenstra is slit-shaped and blocked by lateral wall of maxilla from lateral view. A discrete rounded promaxillary fenestra is present in *Acrocanthosaurus* (*Eddy & Clarke, 2011*), *Marshosaurus* (*Madsen, 1976b*), and some coelurosaurs (Xu et al., 2006; Brusatte et al., 2009). The promaxillary and maxillary fenestrae seem to merge into one opening in Carcharodontosaurinae (*Hendrickx et al., 2015*).

The ventral margin of the maxilla is slightly convex, with one row of neurovascular foramina aligning right above and in parallel with it, similar to those present in *Sinraptor* (*Currie & Zhao, 1993*), *Allosaurus* (*Madsen, 1976a*), and *Monolophosaurus* (*Brusatte et al., 2010a*), in contrast to two rows of neurovascular foramina present in *Marshosaurus* (*Madsen, 1976b*), *Shaochilong* (*Brusatte et al., 2010b*), and *Eocarcharia* (*Sereno & Brusatte, 2008*). The foramina dorsal to the anterior four alveoli opens anteroventrally, then the orientation of subsequent foramina gradually turns more posteroventrally. Each foramina opens ventrally into a depression but is less extensively than the band-like depress in *Ceratosaurus* (*Madsen & Welles, 2000*). After the 10th alveolus, the foramina merge into a discontinuous longitudinal groove.

12 and 10 functional teeth are preserved on the left and right maxilla, respectively. Based on the vacant space, each maxilla is estimated to bear at least 14 alveoli, similar to the condition in many Allosauroids (*Currie & Zhao, 1993*; *Madsen, 1976a*; *Dong et al., 1983*). Each tooth is mediolaterally compressed and strongly curved backward. Both mesial and distal carinae are serrated, and the well-preserved nineth maxillary tooth bears 15 and 20 denticles per 5 mm on the distal and mesial carinae, respectively (Fig. 4 D). The distal carina continues to the base of the crown, but the mesial carina reaches less than half length of the crown from the tip, which is a common condition in theropod. Among these preserved functional teeth, the fourth tooth is the biggest in both left and right maxillae and reach the axial length of 4.60 cm in left and 3.99 cm in right. The 3rd tooth of the premaxilla, which is the biggest premaxillary tooth, is similar in size to the first maxillary tooth, and manifests that the size of the teeth is continuous from the premaxilla to the maxilla. This case differs from the noticeable reduction in size of the posterior premaxillary teeth in Spinosauridae.

Lacrimal—The right lacrimal is preserved relatively complete (Fig. 5 A, B), whereas the left one lacks most of its dorsal part (Fig. 2 A, B). The dorsoventrally height of the lacrimal is 12.08 cm. The ventral ramus of lacrimal contacts the anterodorsal process of jugal, and forms most of the anterior rim of the orbit. The transverse width of the ventral process constricts at its mid-height, and expends anteroposteriorly through the rest ventral part until it sutures with jugal. The posteroventral margin of antorbital fenestra is broken, so it impossible to determine whether the lacrimal contacts the maxilla. The angle between disconnected ventral ramus of lacrimal and the jugal ramus of maxilla is approximately 120° (Fig. 2 C, D), such a blunt angle might be caused by the preservation. The anterior ramus lacks most of its anterior end, but the posterodorsal margin of antorbital fenestra is preserved. The remnant base of the anterior ramus and ventral ramus meet at an angle slightly more than 90°.

The ventral ramus is formed by two laminae as in most other tetanurans: the lateral and the medial. The ridge defined by the boundary of these two laminae forms the posteroventral margin of the antorbital fossa and continues to the jugal. The lateral lamina protrudes anteriorly into the antorbital fenestra at the 2/3 height of the ventral ramus, and separates the antorbital fossa on lacrimal into dorsal and ventral part as in *Allosaurus* (*Madsen, 1976a*), *Monolophosaurus* (*Brusatte et al., 2010a*), and *Acrocanthosaurus* (*Currie & Carpenter, 2000*). In contrast, in *Torvosaurus* (*Britt, 1991*) the antorbital fossa is continuous on anterior and ventral ramus of lacrimal.

The posterodorsal part of the lacrimal bears a small, blunt, triangular boss, which lengthened 2.23 cm with rugosity distributed on its dorsal and ventral lateral surface, proportionally larger than the small boss seen in *Torvosaurus* (*Britt, 1991*), but much less prominent than the distinct lacrimal horn of *Allosaurus* (*Madsen, 1976a*) and *Ceratosaurus* (*Madsen & Welles, 2000*). A weak flange is right below the posterodorsal boss of lacrimal, resembling that of *Ceratosaurus* (*Madsen & Welles, 2000*) and *Sinraptor* (*Currie & Zhao, 1993*). In many carcharodontosaurids (*Acrocanthosaurus*, *Giganotosaurus*, *Mapusaurus*:*Eddy & Clarke, 2011*; *Coria & Salgado, 1995*; *Coria & Currie, 2006*) this flange is more pronounced and forms a process, which marks the lower limit of the eye socket.

Two pneumatic openings excavate the main posterodorsal body of the lacrimal, located at the posterodorsal rim of antorbital fossa. And a third foramen is about 0.8 cm below the larger posterior opening, and falls within the region of antorbital fossa. This combination of foramina is also seen in *Allosaurus* (*Madsen, 1976a*).

Jugal—The anterodorsal border of jugal are broken on both left and right sides, so it is unclear whether the jugal separates the maxilla and lacrimal and slightly contributes to the antorbital fenestra. The remnant jugal is 17.42 cm long on left (Fig. 5 G, H) and 16.40 cm on right side (Fig. 5 C-F). The anterior ramus of jugal rises dorsally into the lacrimal ramus to contact the lacrimal, and contributes to the anteroventral rim of orbit. Immediately posterior to the base of the anterior ramus the postorbital ramus of jugal is 7.02 cm high from the bottom of orbit on the right side, and contributes to the posteroventral margin of the orbit. The postorbital ramus rises abruptly, forms a steep angle with the jugal body. These two rami result in an acute ventral margin of the orbit, similar to the condition in *Sinraptor* (*Currie & Zhao, 1993*), *Yangchuanosaurus* (*Dong et al., 1983*), and *Allosaurus* (*Madsen, 1976a*). Beneath the ventral rim of the orbit, the dorsoventral depth of jugal is 3.3 cm on the left and 2.91 cm on the right.

Posteriorly, the quadratojugal ramus of jugal bifurcates into an upper branch overlapping the anterior ramus of the quadratojugal and a lower branch lying below the quadratojugal as in most theropod, but differs from the triradiate posterior ramus of *Sinraptor* (*Currie & Zhao, 1993*). In better preserved right jugal (Fig. 5 D), the upper branch is slightly shorter than the lower branch, which differs from the much shortened upper branch seen in *Allosaurus* (*Madsen, 1976a*) and *Monolophosaurus* (*Brusatte et al., 2010a*). The quadratojugal ramus strongly turns upwards on the right side, and results in the convex ventral rim of lateral temporal fenestra. This exaggerating curvature is more likely the distortion caused by compression. In contrast, on the left side the quadratojugal ramus curves slightly downwards near the tip of the upper and lower branches (Fig. 5 G, H).

The posteroventral rim of the antorbital fossa is well-developed on jugal, and the rim is demarcated by a ridge which is continues onto the ventral ramus of lacrimal. At the base of this ridge, the lateral surface of jugal is smooth, and differs from the pneumatic openings seen in *Sinraptor* (*Currie & Zhao, 1993*) and Monolophosaurus (*Brusatte et al., 2010a*). Beneath the postorbital ramus, near the bottom of the left jugal, the lateral surface is penetrated by a small and flat foramen (Fig. 5 H), but this foramen is absent on the right side. This might be considered as break, but a similar foramen is present in *Sinraptor*.

Quadratojugal—Both left and right quadratojugals are preserved, the left one (Fig. 5 C-F) is of heavy damage on its lateral surface, while the right one (Fig. 5 I) lacks most of its dorsal ramus. The quadratojugal is L-shaped in lateral view, and compressed mediolaterally as in most theropods. The left quadratojugal is 11.88 cm long and 6.48 cm high, while the right one is 12.96 cm long and 0.73 cm thick.

In lateral view, the ventral margin of the quadratojugal is convex, similar to the condition in *Ceratosaurus* (*Madsen & Welles, 2000*) and *Sinraptor hepingensis* (*Gao, 1992, 1999*). The posterior end of the bone forms a triangular process oriented posteriorly. The lateral surface of the quadratojugal is smooth, with a slight depression (Fig. 5 C, D) extending throughout the base of the dorsal ramus and occupy roughly 2/3 ventral depth of the main body. The anterior process tapers anteriorly and is wedged into the upper and lower branches of the posterior ramus of the jugal. The anterior process extends to be level with the anterior border of the lateral temporal fenestra, more anteriorly than those of *Allosaurus* (*Madsen, 1976a*) and *Sinraptor dongi* (*Currie & Zhao, 1993*), but falls shorter than the condition in *Monolophosaurus* (*Brusatte et al., 2010a*). The dorsal process is preserved on the left quadratojugal, but most of its external surface is broken. The remnant dorsal process takes the form of triangular, and tapers dorsally. The articulation with the squamosal is not definitive due to the latter's missing.

In the medial view, the posterior end of the quadratojugal bears slight rugosity, which might be the contact with the quadrate as in *Allosaurus*. Anterior to this rugosity, a deep fossa excavates into the posterior end with a rounded rim (Fig. 5 E, F), and the bony wall is thin as a lamina corresponding to the concave lateral surface.

Postorbital—Only the right postorbital has been preserved, and lacks most distal part of its posterior ramus (Fig. 6 A, B). In lateral view, the postorbital is T-shaped in outline consisting of the orbital, posterior and ventral rami. The postorbital measures 9.83 cm in dorsoventrally height and 6.17 cm in anteroposteriorly length from the orbital ramus to the broken base of the posterior ramus.

The postorbital projects anteriorly to form a sheet-shaped process (Fig. 6 A, B), differing from the prominent orbital boss as seen in other derived metriacanthosaurids (*Dong et al., 1978, 1983*; *Gao, 1992*; *Currie & Zhao, 1993*; *Rauhut et al., 2024*). From the beginning of the juncture of orbital ramus and ventral ramus of the postorbital, the orbital ramus is 2.69 cm long. Through this planar orbital ramus, the postorbital contacts the frontal medially, and forms the orbital roof along with prefrontal, lacrimal and a slight part of frontal as in *Sinraptor* (*Currie & Zhao, 1993*) and *Allosaurus* (*Madsen, 1976a*). In contrast, the frontal or prefrontal is excluded from the orbital rim due to the postorbital-lacrimal articulation as in *Carcharodontosaurus* (*Sereno et al., 1996*) and *Eocarcharia* (*Sereno & Brusatte, 2008*). The orbital ramus maintains a relatively constant thickness with the deepest portion measured 0.99 cm. This constant thickness of the orbital process of postorbital in *Yuanmouraptor* also differs from conditions in *Torvosaurus* (*Britt, 1991*) and *Eustreptospondylus* (*Sadleir et al., 2008*), in which the orbital processes increase the dorsoventral depth gradually backwards.

The ventral ramus of the postorbital is transversely widened and anteroposteriorly tapered to the distal end, with a prominent lamina (Fig. 6 A-D) running along its posterior border, differing from the U-shaped posterior rim of postorbital in many megalosauroids (*Torvosaurus*; *Eustreptospondylus*; *Wiehenvenator*: *Britt, 1991*; *Sadleir et al., 2008*; *Rauhut et al., 2016*). Through the ventral part of this lamina the postorbital contacts the postorbital ramus of jugal. The upper half of the ventral ramus extends posteroventrally, then the lower half turns downwards with its tip curves backwards, resulting in gently sigmoidal profile in lateral view. The anterior rim of the ventral ramus is smooth and concave, and there is no evidence of any anteriorly projecting intraorbital process which defines the ventral border of eyeball as in *Acrocanthosaurus* (*Eddy & Clarke, 2011*), *Carcharodontosaurus* (*Sereno et al., 1996*), *Majungosaurus* (*Sampson & Witmer, 2007*). A shallow trough begins at the anterodorsal rim of the orbit, then twists to face laterally on the ventral ramus and shallows ventrally, which is considered as an autapomorphy of *Yuanmouraptor*.

The roof of the postorbital body expands laterally into a longitudinal ridge, ventral to which the lateral surface of main body forms a shallow depression (Fig. 6 B). This longitudinal ridge continues onto the posterior ramus of postorbital, and marks the lateral rim of the supratemporal fossa. The remnant of posterior ramus is mediolaterally thin, and its cross section tapers dorsolaterally to form the ridge. The posterior ramus is deflected at an angle of nearly 70° from the posteroventrally pointed ventral ramus.

In dorsal view (Fig. 6 E, F), a medial process contacts frontal anteriorly and laterosphenoid posteromeidally, forms the anterolateral border of the supratemporal fenestra. Between the frontal and laterosphenoid, this process also has a very limited contact with the lateral projection of parietal, similar to the condition of *Sinraptor* (*Currie & Zhao, 1993*). The supratemporal fossa is shown as a shallow, poorly-defined depression, and its anterior rim is formed by postorbital together with frontal, parietal and laterosphenoid.

Prefrontal—The prefrontal is a small element located between lacrimal and frontal, partly lacks its anterior end (Fig. 6 E, F). The remnant prefrontal measures 5.15 cm in lenghth, 2.70 cm in width and 1.88 cm in depth. Due to the damage, the prefrontal is displaced posteriorly relative to frontal, and overlapps the mediodorsal surface of the lacrimal. The nasal is poorly preserved, thus the articulation between the prefrontal and the nasal is not definitive.

In dorsal view, the frontal is sub-rhomboid in outline, and contacts lacrimal laterally and frontal medially, but sutures of these articulations are all broken. The dorsal surface of prefrontal is planar and smooth. The prefrontal's posterolateral rim, which contributes to the orbital roof, is slightly rugose as in *Sinraptor* (*Currie & Zhao, 1993*), this rugosity might continue onto the lacrimal boss. Unlike the fusion with other bones or lateral covering of the lacrimal in carcharodontosaurids and ceratosaurs (*Sereno et al., 1996*; *Sereno & Brusatte, 2008*; *Sampson & Witmer, 2007*), the prefrontal of *Yuanmouraptor* is exposed laterally on the dorsal rim of orbit and forms a supraorbital notch together with frontal, postorbital and lacrimal, a condition close to that in *Allosaurus* (*Madsen, 1976a*), *Sinraptor* (*Currie & Zhao, 1993*), and *Monolophosaurus* (*Brusatte et al., 2010a*).

Frontal—The paired frontals (Fig. 6 E, F) are wedge-shaped in outline in dorsal view, and articulate each other through the suture on the midline, though the structure of this suture is deformed due to the compressional distortion. Both left and right frontals are preserved, but lack their anterior end, thus the articular surface with nasal is not definitive. The right frontal is relatively complete, about twice as long as it is wide, and measures 10.82 cm in length and 5.77 cm in width. Whereas the left frontal lacks its posterolateral part.

In dorsal view, the frontal contacts the prefrontal anteromedially, the postorbital posterolaterally and the parietal posteromedially. The frontal reaches its great mediolateral width at a point level with its contact with the postorbital, resembling that in *Sinraptor* (*Currie & Zhao, 1993*) and *Allosaurus* (*Madsen, 1976a*). In contrast, the frontal of *Eustreptospondylus* (*Sadleir et al., 2008*) is widest at the supraorbital notch. Prior to the contact with the postorbital, the transverse width of the frontal shrinks abruptly to contribute to the supraorbital notch, this also occurs in *Sinraptor* and *Allosaurus*. At the anterior rim of the supraorbital notch, the frontal expands laterally to form the contact with the prefrontal, then the frontal tapers anteriorly. The dorsal surface of the frontal is smooth, and its posterolateral part was occupied by a poorly-defined shallow recess, which is continues with the recess on the postorbital and contributes to the anterior rim of supratemporal fossa. Although the suture between paired frontals is broken, there is no sign of a midline ridge as displayed in *Shaochilong* (*Brusatte et al., 2010b*). Posteriorly, the suture with the parietal is interdigitating medially and roughly straight laterally, resembles that of *Sinraptor*, *Allosaurus* and *Shidaisaurus* (*Wu et al., 2009*).

Parietal—The paired parietals are fused, and lack most of their posterodorsal part (Fig. 6 E, F). The remnant parietal is similar to that of *Sinraptor* (*Currie & Zhao, 1993*) and *Shidaisaurus* (*Wu et al., 2009*) in outline, and measures 6.69 cm in length and 8.24 cm in width. In dorsal view, the parietal contacts the frontal through an interdigitating suture anteriorly. Posterior to the contact with the frontal, the parietal expands laterally to form two slender projections, contacting the posterolateral part of frontal in transversely straight suture. The tips of these projections reach the postorbital and overlap the laterosphenoid. The dorsal surface between the projections is dorsally convex, and differ from the additional bone deposition which protrudes laterally into the supratemporal fenestra as in *Sinraptor*. Behind these projections the parietal constricts transversally and measures as 2.84 cm in width. Due to the serious damage present on the posterodorsal part of the parietal, the existence of nuchal crest and the border between the parietal and the supraoccipital is not definitive.

Squamosal—Only the right squamosal has been preserved (Fig. 7 A-E), but deviates strongly from the original position, with its anterior and ventral end obscured by sediment. As in many theropods, the squamosal of *Yuanmouraptor* comprises four processes: the anterior process contacting the posterior ramus of the postorbital; the ventral process that extends ventrally to cover the quadrate laterally and contact the ascending process of quadratojugal; the medial process underlapping the parietal; and a posterior process that envelopes the paroccipital process anterolaterally.

In dorsal view (Fig. 7 A, B), the preserved part of squamosal measures 6.24 cm in maximum length and 6.62 cm in width. The dorsal surface of the squamosal is smooth and slightly concave, and subtriangular in outline. The obscuration of the postorbital and sediment preclude the observation of the medial border of the dorsal surface of the squamosal, which contributes to the posterolateral rim of the supratemporal fenestra. The lateral rim of dorsal surface is demarcated by a ridge (Fig. 7 B) which extends posteriorly from the remnant of the anterior process then recurves medially at the base of the posterior process. The articular surfaces for the parietal and the paroccipital together form the posterior border of the squamosal (Fig. 7 D). The medial process protrudes anteromedially and is slightly convex posteromedially. The coarse surface of the medial process, which is not continuous with the dorsal surface of the bone, indicates its contact with the parietal. Anteromedial to the posterior process, the articular surface for the tip of the paroccipital process is posteriorly concave and dorsoventrally deep, then becomes posteriorly flat and constricts in depth to continue onto the base of the medial process.

In lateral view (Fig. 7 E), the remnant anterior process measures 3.36 cm in length, bears evident dorsal and ventral rim, and the former contributes to the border of the concavity on the dorsal surface. The remnant ventral process measures 3.25 cm in depth and inclines anteroventrally. Together the anterior and ventral processes of the squamosal form the posterodorsal rim of the lateral temporal fenestra, these two processes are at an angle of broadly 70°. In contrast, this angle is blunter in basal-branching tetanurans such as *Sinraptor* (*Currie & Zhao, 1993*), *Allosaurus* (*Madsen, 1976a*), *Afrovenator* (*Sereno et al., 1994*), and *Eustreptospondylus* (*Sadleir et al., 2008*). The tip of the posterior process projects 1.89 cm posteriorly from the main body of the squamosal, and differs from the posteroventrally oriented posterior process of *Sinraptor* (*Currie & Zhao, 1993*), *Allosaurus* and *Monolophosaurus* (*Brusatte et al., 2010a*). The lateral surface of the posterior process of the squamosal is rugose and pitted, might for the attachment of ligament.

In posterior view (Fig. 6 C, D), the squamosal is dorsoventrally deep along the contact with the exoccipital, and reaches its maximum depth near the posterior process, but becomes shallow toward its medial process. The bottom of the articulate surface for the paroccipital process is concave ventrally, might houses the quadrate head.

Quadrate—Both the left and right quadrate are seriously damage, the former (Fig. 7. F-H) lacks most of its dorsal part and the latter (Fig 2. D) only preserves partial pterygoid flange. The bottom of the left quadrate is well-preserved, with measuring 4.69 cm in mediolateral width, and is separated by an anteromedially oriented intercondylar sulcus into the entocondyle and the ectocondyle (Fig. 7 H). The ectocondyle is larger, which is similar to the condition in *Allosaurus*, but contrasts with that of *Eustreptospondylus* (*Sadleir et al., 2008*) and *Ceratosaurus* (*Madsen & Welles, 2000*) in which the entocondyle is rather larger. The ectocondyle is 2.79 cm wide mediolaterally while the entocondyle is 2.5 cm wide. The long axes of the ento- and ectocondyles are anteromedially oblique in broadly same direction, but slightly more medially directed than the degree of the intercondylar sulcus. The anterior end of each condyle is at approximately the approximate level, which contrasts with the strongly anterior protruding entocondyle in *Torvosaurus* (*Britt, 1991*) and *Eustreptospondylus*. In lateral view, both mandibular condyles extend anteriorly to form a concavity dorsal to them, while the posterior rim of the remnant quadrate is straight along the shaft.

Palatine—The incomplete left palatine is preserved (Fig. 7 I, J) and lacks most of its posterior processes, with its medial surface obscured by matrix. Whereas the right palatine is present by a bar-like bone, and its structure is impossible to identify. The palatine takes the form of a saddle, with the central part of the bone is lowest in dorsoventral depth. As preserved the palatine is 11.23 cm long anteroposteriorly, 4.5 cm deep dorsoventrally at the vomeropterygoid process, and 2.64 cm deep at the waisted region of the main body.

The anterior vomeropterygoid and maxillary processes are preserved, together define the posterior limit of the internal naris choana. The vomeropterygoid process lacks its distal end, and inclines mediodorsally at its base, then becomes more anteriorly oriented, thus the medial rim of the coana is concave laterally. The maxillary process is more robust than the vomeropterygoid process, and extends anteriorly with a laterally convex surface. The articular surface with the maxilla of the palatine is not definitive due to the damage. In lateral view, a shallow fossa is present at the base of the maxillary process, immediately posterior to the internal naris choana. This fossa might mark the pneumatic recess of palatine, but does not penetrate the surface of bone and lead to the inner space as in *Sinraptor* (*Currie & Zhao, 1993*) and *Acrocanthosaurus* (*Eddy & Clarke, 2011*). A similar fossa is present in *Neovenator* (*Brusatte et al., 2008*), but it is located more posteriorly at the juncture of the jugal and medial process.

Supraoccipital—The supraoccipital is seriously broken, with most of its dorsal part missing. The preserved part of the supraoccipital (Fig. 8 A, B) is 2.73 cm deep dorsoventrally and 5.19 cm wide transversely at its base. Despite the heavy damage, the preserved base of the supraoccipital indicates a prominent ridge running on the midline, and flanked by a pair of vertical grooves. Lateral to the paired grooves the bone extends posterolaterally and might continue onto the probable nuchal crest of parietal. The base of the middle ridge is triangular in shape, tapers dorsally, and expands transversely based on the dorsal fracture. The ventral rim of supraoccipital makes a slight contribution to the dorsal border of the foremen magnum as in *Sinraptor* (*Currie & Zhao, 1993*), *Acrocathosaurus* (*Eddy & Clarke, 2011*), *Monolophosaurus* (*Zhao & Currie, 1993*), and *Piatnitzkysaurus* (*Rauhut, 2004*), and this contribution measures 0.83 cm in breadth. On the left side of the base of the bone, there are two foramina penetrates the external surface, but on the opposite side the surface is smooth. The symmetrical paired foramina positioned lateral to the midline near the base of supraoccipital are generally referred as exits for external occipital vein (*Currie & Zhao, 1993*), vena capitis dorsalis (*Coria & Currie, 2002*; *Rauhut, 2004*; *Brusatte & Serreno, 2007*; *Eddy & Clarke, 2011*) or vena cerebralis media (*Sampson & Witmer, 2007*). The asymmetrical foramina present in supraoccipital in *Yuanmouraptor* might be caused by pathology or taphonomic process. The supraoccipital expands laterally at its ventral margin to contact otoccipitals.

Otoccipital (Exoccipital-Opisthotic) —The main body of the exoccipital-opisthotic complex is well-preserved, but the tips of left and right paroccipital processes are missing (Fig. 8 D, E). A possible suture between the exoccipital and opisthotic is present. In all preserved vertebrae the neural arch is attached to the centrum and the absence of neurocentral suture in most of them, indicating that this individual is nearly mature or subadult, thus this suture-like boundary is more likely caused by damage.

In posterior view (Fig. 8 D, E), the paired exoccipitals are separated by the supraoccipital above the foramen magnum. Then the exoccipitals form the lateral and ventral margin of the foramen magnum, and meet each other at a midline suture throughout the dorsal surface of the occpital condyle. The foramen magnum is 2.47 cm transversely wide and 1.32 cm dorsoventrally high, proprotionally broader than that of *Sinrapor* (*Currie & Zhao, 1993*) and *Allosaurus* (*Madsen, 1976a*). The paroccipital process is posterolaterally directed, and slightly turns downwards, contrasts more sharply downturned condition with *Sinrapor* (*Currie & Zhao, 1993*) and *Allosaurus* (*Madsen, 1976a*). The ventral limit of the base of process levels with the bottom of the occipital condyle, as in *Allosaurus*, *Sinraptor*, and *Piatnitzkysaurus* (*Rauhut, 2004*), but contrasts more dorsally placed ventral base of the paroccipital process with *Dubreuillosaurus* (*Allain, 2002*), *Eustreptospondylus* (*Sadleir et al., 2008*), and *Leshansaurus* (*Li et al., 2009*). A depressed area (Fig. 8 C) lies between the paroccipital process and the base of occipital condyle, and houses three foramina for cranial nerves. Among these foramina, the dorsal one is for the vagus (X) and accessory (XI) cranial nerves, the medioventral one and the lateroventral one is for the two branches of the hypoglossal nerve (XII). The ventral part of the exoccipital-opisthotic tapers ventrally, and overlaps the basioccipital laterally at the boundary between the basioccipital and the basisphenoid. The suture with the basioccipital extends from the base of the occipital condyle to the basal tubera.

In lateral view (Fig. 9 A, B), the anterodorsal corner of the exoccipital-opisthotic is coverd by the prootic, and the exoccipital-opisthotic forms the posterior boundary of the fenestra ovalis approximately ventral to the crista prootica. The posteroventral rim of the paroccipital process, formed by the metotic strut, is strongly concave posteriorly, and separates lateral and posterior surfaces of the braincase. The suture with the basisphenoid is posteroventrally inclined and slightly posteriorly concave.

Prootic—The prootic is mainly exposed on the lateral surface (Fig. 9), and the right prootic is better preserved than the left one, with a complete prootic pendant. The prootic contacts the laterosphenoid anteriorly, and posterior to the contact a shallow recess is present. Ventral to the suture with the laterosphenoid, a longitudinal groove runs through the ventral part of the prootic. Approximately posterior to the groove, a single foramen penetrating the bone houses the cranial nerve VII, differs from two openings for the cranial nerve VII in *Eustreptospondylus* (*Sadleir et al., 2008*). The opening for trigeminal (V) nerve originates in the anterior-most part of the prootic and is even bounded by the laterosphenoid anteriorly in many tetanurans such as *Sinraptor* (*Currie & Zhao, 1993*), *Eustreptospondylus*, *Dubreuillosaurus* (*Allain, 2002*), *Monolophosaurus* (*Brusatte et al., 2010a*), and *Piatnitzkysaurus* (*Rauhut, 2004*), but in *Yuanmouraptor* this part is obscured by the sediment, preventing the further observation.

The prootic contact the exoccipital-opisthotic posteroventrally with a jagged suture. A prominent crista prootica (Fig. 9 B) marks the posteroventral margin of the prootic. Above the crista prootica the prootic is contiguous with the base of paroccipital process and overlaps the exoccipital-opisthotic laterally. The prootic forms the anterior boundary of the fenestra ovalis with the exoccipital-opisthotic forming the posteroventral boundary, approximately ventral to the crista prootica. Anteroventral to the fenestra ovalis, a slight process sits at the boundary between the exoccipital-opisthotic and basisphenoid, and protrudes posteroventrally, similar to that in *Sinraptor*.

The ventral part of the prootic mainly overlaps the basisphenoid laterally with the prootic pendant, and the space between the pendant and exoccipital-opisthotic is infilled by sediment.

Basioccipital—The basioccipital is mainly exposed in the posterior view (Fig. 8 D, E), and its central ventral part is incomplete. The basioccipital occupies more than 60 percent of the occipital condyle. The occipital condyle is evidently wider (3.28 cm) than tall (2.3 cm), with rounded and smooth articular surface. Unlike in *Sinraptor* (*Currie & Zhao, 1993*), *Allosaurus* (*Madsen, 1976a*), and *Eustreptospondylus* (*Sadleir et al., 2008*), the basioccipital of *Yuanmouraptor* does not contribute to the foramen magnum, and the paired exoccipitals meet each other in the midline. Ventral to the neck of the occipital condyle, a shallow fossa is present, and the surface below the neck is posteriorly concave and smooth, but is not as well-defined as the subcondylar recess seen in *Piatnitzkysaurus* (*Rauhut, 2004*). The ventral rim of the basioccipital on the right side probably represent the basal tuber, though it is not very apparent due to the damage. The remnant basal tuber is level with the ventral limit of exoccipital-opisthotic, in contrast to the unusual condition of *Sinraptor*, in which the exoccipital-opisthotic extends significantly more ventrally than the basal tubera. Differs from the relatively narrow width between the basal tubera in *Sinraptor*, *Allosaurus*, and *Monolophosaurus* (*Zhao & Currie, 1993*), the transverse width across the basal tubera is broader than the transverse diameter of the occipital condyle in *Yuanmouraptor*. The suture with the basisphenoid is visible near the basal tubera and could only be observed on the right side.

Basisphenoid—The basisphenoid could be mainly observed on the right side (Fig. 9). Its ventral structures such as the basisphenoid recess and the basipterygoid process are obscured by other bones and sediment. In lateral view, the basisphenoid contacts the exoccipital-opisthotic through a posteriorly curved suture. The suture with the basioccipital is visible on the tip of the basal tubera. The dorsal part of the basisphenoid is overlapped by the prootic. Only the base of the cultriform process is exposed, and the remnant of it is obscured by matrix.

Laterosphenoid—Both left and right laterosphenoids are preserved, but most of their ventral parts are either damaged or obscured by matrix. The laterosphenoid forms the anterior wall of the brancase, and is surrounded dorsally by the parietal, posteriorly by the prootic and laterally by the postorbital. The contact with the forntal is not definitive due to the bloking of the surrounding articulated bones. The laterosphenoid is visible in dorsal and laterodorsal views(Figs 6, 9), and forms the anteromedial rim of the supratemporal fenestra.

Dentary—Dentaries are preserved on both left and right side, but their posterior boundaries are broken, so the suture with the surangular and angular is not clear. The relatively complete right dentary (Fig. 2 C, D) is 34.1 cm long and reaches minimum depth (4.17 cm) at the level of the fourth alveolus. In lateral view, the main part of the upper margin is straight, but a step appears at nearly the fourth dentary teeth leading to a slight dorsoventral expansion as in *Eustreptospondylus* (*Sadleir et al., 2008*). In contrast to the square anteroventral rim of dentary in *Giganatosaurus* (*Coria & Salgado, 1995*), the tip of the ventral rim of dentary in *Yuanmouraptor* is rounded. The lower margin of the dentary is concave and inclines more ventrally at the 11th alveolus, posterior to which the dentary body expands vertically throughout its posterior half length. An array of slightly undulate neurovascular foramina (Fig. 10 A, B) excavates the external surface of the bone below anterior seven tooth. Posterior to and level with these foramina, a longitudinal groove extends from the 11th alveolus along the rest dentary and runs upward gradually. Several smaller foramina scatter over the anteroventral margin of the lateral surface. The function of these neurovascular foramina on the dentary might be the same as those on the premaxilla and maxilla. Most of the left and the right dentaries adhere to the matrix or other bones, only a bit of medial surface of the left dentary is observable but poorly-preserved (Fig. 2 D). Through this limit expose of medial surface, two unfused interdental plates are preserved on the exposed medial surface, and takes form of sub-triangular, as in *Sinraptor* (*Currie & Zhao, 1993*), *Dubreuillosaurus* (*Allain, 2002*), *Marshosaurus* (*Madsen, 1976b*), and *Eustreptospondylus* (*Sadleir et al., 2008*). Ventral to the interdental plates a trough represents the paradental groove, which demarcates the ventral border of the interdental plates. A replacement tooth occurs between these two interdental plates, and an unerupted tooth is exposed on the broken surface near the damaged interdentary symphysis, exhibiting serrated distal carina. The Meckelian groove appears as a narrow trough on the remnant dentary, and the foramina anterior to it as in *Sinraptor* (*Currie & Zhao, 1993*) and *Allosaurus* (*Madsen, 1976a*) might be damaged.

The relatively well-preserved left dentary (Fig. 10. A, B) bears nine functional teeth, from gaps among which, at least 14 alveoli are estimated. 14-17 teeth are present in other derived Late Jurassic allosauroids such as *Sinraptor* (*Currie & Zhao, 1993*), Y*angchuanosaurus* (*Dong et al., 1983*), and *Allosaurus* (*Madsen, 1976a*). Similar to the condition in maxillary teeth, the distal carina of dentary teeth continues form the base to the tip while the mesial carina develops along less than half of the teeth from the apex. The dentary teeth are generally smaller in size than maxillary tooth with the largest dentary teeth measures 2.73 cm high. Dentary teeth also have greater curvature than those of maxillary and premaxillary teeth.

Splenial—Only the right splenial is observable, and is poorly-preserved, with most of its anterior part obscured by other elements and the posterior boundary damaged (Fig. 10 E, F). Caused by the compression during burial, the bone covers the anterior end of the prearticular medially. The bone forms a posteroventrally tapering process and its anteroventral rim is slightly concave and smooth.

Surangular—The left surangular (Fig. 10 C, D) are better preserved than the right one, while the latter is heavily compressed dorsoventrally, and the anterior end of each one are obscured or damaged (Fig. 2). The right surangular measures 27.26 cm anteroposteriorly, and its suture with the dentary is not clear due to the compression.

Anterolateral to the contact with the articular, a longitudinal surangular ridge (Fig. 10 D) is present approximately below the dorsal margin of the surangular. The ridge ends posteriorly with a dorsal concavity, which laterally demarcates the lateral glenoid contacting the ectocondyle of the quadrate. Posterior to the lateral glenoid the surangular forms a U-shaped notch deeper than the lateral glenoid, which contributes to the retroarticular process together with the articular, and is similar to but dorsoventrally deeper than that of *Sinraptor* (*Currie & Zhao, 1993*) and *Acrocanthosaurus* (*Eddy & Clarke, 2011*). The posterolaterally opened posterior surangular foramen is exhibited posteroventrally to the surangular ridge and ventrolaterally to the mandibular joint, and a second foramen is found further anteriorly. This resembles that of *Sinraptor* but contrasts with the condition in *Monolophosaurus* (*Brusatte et al., 2010a*), in which the surangular ridge is absent and the posterior surangular foramen is roofed by an unexpanded and smooth surface.

The surangular forms most of the dorsal and posterior rim of the external mandibular fenestra. At the posteroventral corner of the external mandibular fenestra, the surangular is overlapped laterally by the bony wall formed by the angular. Medially the surangular have a hook like process (Fig. 10 E, F), which forms an angle of nearly 60° with the long axis of the surangular and contacts the prearticular ventrally (Fig. 11 C, D). The posterior rim of the hooked process extends laterally and contributes to dividing the glenoid into two parts. In medial view (Fig. 10 E, F), the surangular thickens transversely to form a bar like dorsal rim, which demarcates the dorsal limit of the adductor fossa. The M. adductor mandibulae externus is estimated to attach the concave surface between this bar and the surangular ridge.

Angular—The left angular lacks most of its anterior part (Fig. 10 C, D), and the right angular is strongly dorsoventrally compressed. The angular forms the posteroventral part of the mandible, it thins dorsally to cover the surangular, and thickens ventrally to overlap the ventral margin of the prearticular, which forms the ventral border of the adductor fossa. The angular is dorsally concave, and forms the ventral rim of the external mandibular foramen. The remnant angular reaches the maximum depth at its central part of the contact with the surangular.

Prearticular—The right prearticular could be observed in medial view (Fig. 10 E, F). The bone is a ventrally bowed element, it dorsoventrally flares at its anterior and posterior ends, but constricts in depth at its central part. The medial surface of the remnant prearticular is obscured by angular anteriorly and surangular posteriorly. The anterior part of the ventral rim of the prearticular is surrounded ventrally by the thickened angular. Whereas posterior to the contact with the angular, the ventral rim of the angular is exposed in lateral view as in *Sinraptor* (*Currie & Zhao, 1993*) and *Acrocanthosaurus* (*Eddy & Clarke, 2011*). The posterodorsal part of the prearticular forms a dorsomedially directed triangular process, which contacts the hooked process of surangular dorsolaterally (Fig. 11 C, D). Posterior to this process the prearticular forms a dorsally concave embayment, which houses the articular.

Articular—The right articular is well-preserved and still in articulation with the prearticular and surangular (Fig. 11). The retroarticular process is well-developed and has a concave dorsal surface, which is dorsally oriented and bordered by sharp ridge, in contrast, this surface faces more posteriorly in *Allosaurus* (*Madsen, 1976a*) and *Acrocanthosaurus* (*Eddy & Clarke, 2011*). In lateral view (Fig. 11 A, B), the lateral rim of the retroarticular process surpasses the lateral wall of the surangular and exposes laterally. In dorsal view, the posterior end of the retroarticular process is U-shaped in outline, then the process constricts its lateral rim abruptly and then expands medially at its anterior part, forming a lateral notch and a medial blunt process. This medial blunt process is contiguous with the medial rim of the medial glenoid, and the opening for the chordra tympani penetrates it from its posterodorsal surface to its ventral surface. Anteriorly a prominent ridge separates the medial glenoid and retroarticular process as in *Sinraptor* (*Currie & Zhao, 1993*), this ridge is more eminent in *Acrocanthosaurus* (*Eddy & Clarke, 2011*).

General description of the axial skeleton

All vertebrae are well-preserved but none of them bears a rib. ~~Of them~~ the first 10 vertebrae were considered as belonging to the cervical series ~~and~~ the 11th was speculated to be the first dorsal vertebra based on the common condition of 10 cervical vertebra in basal-branching tetanurans (*Holtz et al., 2004*) and the diapophysis of the eleventh vertebra that is more laterally expanded than the preceding one as is the case in *Sinraptor* (*Currie & Zhao, 1993*) and *Yangchuanosaurus* (*Dong et al., 1983*). The neurocentral suture is only partly visible on the eighth and ninth cervicals, indicating that this individual is an adult or subadult.

Atlas-Axis—In the atlas-axial complex (Fig. 12), the atlantal intercentrum is in articulation with the axial intercentrum and odontoid. The proximal parts of both the left and right neurapophyses are still attached to the atlantal intercentrum and are positioned laterally to the neural canal. There is no evident prezygopophysis on the neurapophysis, indicating the absence of the proatlas as in *Sinraptor* (*Currie & Zhao, 1993*). The exposed part of the atlantal intercentrum is similar to that of *Shidaisaurus* (*Wu et al., 2009*) and *Sinraptor* (*Currie & Zhao, 1993*). In anterior view, the main body of the atlantal intercentrum is slightly wider than deep. The ventrolateral rim is slightly convex, and the ventral rim becomes flat, resulting a sub-rectangular profile of the lower half. The anterior articular surface is concave, for the articulation with the occipital condyle. The dorsal rim of the atlantal intercentrum is ventrally depressed and underlaps the rounded ventral part of odontoid.

The odontoid adheres to the upper half of the anterior articular surface of the axial centrum, and its boundaries with the atlantal intercentrum and axial centrum are visible. The odontoid is divided into a dorsal and an anterior surface by an anteriorly convex rim, and this rim is approximately parallel with the ventral border which contacts the atlantal intercentrum. The dorsal surface of odontoid is dorsally concave and continuous with the floor of the neural canal. The anterior surface arches anteriorly to pass through the dorsal margin of the atlantal intercentrum. A single shallow recess is located laterally on each side of the anterior surface of the odontoid, which differs from the foramina penetrating the same position as these recesses in *Neovenator* (*Brusatte et al., 2008*). In anterior view the odontoid is in shape of semicircle, similar to the condition in *Allosaurus*

(*Madsen, 1976a*) and *Monolophosaurus* (*Zhao et al., 2009*).

The axial intercentrum is not observable in anterior view (Fig. 11 C) due to the obscuration of the articulated atlantal intercentrum. In lateral view (Fig. 11 E), the axial intercentrum tapers posterodorsally to form a sub-triangular lateral outline as in *Neovenator* (*Brusatte et al., 2008*), *Piatnitzkysaurus* (Bonapart, 1986), and *Yunyangosaurus* (*Dai et al., 2020*). In contrast, the axial intercentrum maintains a constant anteroposterior thickness dorsoventrally, resulting a sub-rectangular outline in lateral view in *Sinraptor* (*Currie & Zhao, 1993*) and *Ceratosaurus* (*Madsen & Welles, 2000*). The suture between the axial intercentrum and centrum is slightly inclined anteroventrally, similar to the condition present in *Sinraptor* (*Currie & Zhao, 1993*), but in contrast ~~with~~ nearly vertical suture in *Allosaurus* (*Madsen, 1976a*), *Neovenator* (*Brusatte et al., 2008*), *Piatnitzkysaurus* (Bonapart, 1986), and *Yunyangosaurus* (*Dai et al., 2020*). The ventral surface of the axial intercentrum is flat and ~~ventrally faced, continuous~~ with the ventral surface of the axial centrum in lateral view as in *Ceratosaurus* (*Madsen & Welles, 2000*), *Dilophosaurus* (*Marsh & Rowe, 2020*), *Majungasaurus* (O'Connor, 2009), *Piatnitzkysaurus* (Bonaparte, 1986), and *Yunyangosaurus* (*Dai et al., 2020*), ~~but differs~~ from *Sinraptor* (*Currie & Zhao, 1993*), *Monolophosaurus* (*Zhao et al., 2009*), *Neovenator* (*Brusatte et al., 2008*), and *Acrocanthosaurus* (*Harris, 1998*), ~~in which~~ the ventral surface of the axial intercentrum is nearly horizontal. In ventral view (Fig. 11 B), the suture between the intercentrum and centrum is well exposed and arches anteriorly.

The axial centrum is longer ventrally than it is dorsally, ~~a similar condition~~ in *Sinraptor* (*Currie & Zhao, 1993*). The anterior articular surface is mostly obscured by the odontoid and axial intercentrum. The posterior articular surface is strongly concave, and is ~~as approximately~~ wide as high. In lateral view, the ventral rim of the centrum strongly arches dorsally, and forms an acute angle with the posterior articular surface as in *Sinraptor* (*Currie & Zhao, 1993*). The diapophysis is located at the base of the neural arch, just above the centrum, and is present as a lateroventrally oriented pedicle. Anteroventral to the diapophysis the parapophysis protrudes posteroventrally to form a diminutive hump. The lateral surface of centrum is smooth and there is no trace of any pneumatic structure. This contrasts with many allosauroids (*Currie & Zhao, 1993*; *Brusatte et al., 2008*; *Harris, 1998*), in which pleurocoels invade the main body of the centrum ventral to the diapophysis. The central part of the centrum tapers its transverse width downwards, resulting an mediolaterally narrow and flat ventral surface as is the case in *Yunyangosaurus* (*Dai et al., 2020*). This differs from the centrum that bears pronounced ventral keel in *Acrocanthosaurus* (*Harris, 1998*). The transversely narrow and ventrally tapering ventral surface of axial centrum without ventral keel was considered as an autopomorphy of *Yunyangosaurus* (*Dai et al., 2020*).

The prezygopophyses are obscured by neurapophyses on both left and right sides (Fig. 11 E, F). The postzygopophyseal facets of the axial centrum are well-developed, comparable in size to those of postaxial cervicals. The V-shaped intrapostzygopophyseal lamina (tpol) medially connects ~~paired~~ postzygopophyses dorsal to the neural canal. The developed epipophysis extends posterodorsally from the distal end of the postzygopophysis and curves laterally. A well-developed axial epipophysis also occurs in *Shidaisaurus* (*Wu et al., 2009*), *Sinraptor* (*Currie & Zhao, 1993*). The neural spine is transversely thin and posterodorsal inclined. In lateral view, the neural spine deflects at an angle of 50° with the neural canal throughout its ventral half, then the degree of inclination decreases abruptly in rest dorsal part. ~~This transition in~~ the degree of deflection is probably caused by breakage. Prior to the base of neural spine, a rounded eminence rises dorsally, similar to the condition in *Neovenator* (*Brusatte et al., 2008*) and *Yunyangosaurus* (*Dai et al., 2020*). The anterior end of the neural spine is positioned posterior to the anterior margin of the neural canal, ~~this contrasts~~ the strongly anteriorly flared neural spine in *Dilophosaurus* (*Marsh & Rowe, 2020*). The spinopostzygopophyseal lamina expands laterally from the neural spine and fills the space between its summit and the epipophysis, resembling that of *Sinraptor* (*Currie & Zhao, 1993*; *Gao, 1993*, 1999), *Yangchuanosaurus* (*Dong et al., 1983*), *Dilophosaurus* (*Marsh & Rowe, 2020*), and *Yunyangosaurus* (*Dai et al., 2020*). In posterior view (Fig. 11 D), an anteriorly excavated and subtriangular fossa is surrounded by the spinopostzygopophyseal lamina and postzygopophyses, such fossa also occurs in *Sinraptor* (Currie & Zhao, 1993; *Gao, 1992*, 1999), *Yangchuanosaurus* (*Dong et al., 1983*), *Ceratosaurus* (*Madsen & Welles, 2000*), and *Dilophosaurus* (*Marsh & Rowe, 2020*).

Postaxial vertebrae—The third to fifth cervical centra are opisthoceolous with dorsally arched ventral surface. In remnant elements of the cervical series the anterior articular surface becomes flat or slightly convex, and their corresponding posterior articular surface becomes less concave, resulting the platycoelous centra. The centra of the postaxial cervicals are anteroposteriorly longer than dorsoventrally high, whereas the length/height ratio gradually decreases posteriorly through the cervical series. A distinct rim (Fig. 13 A-C) is present on the anterior articular surface of the anterior cervicals, and it is especially well defined on the third cervical. This distinct rim also occurs on anterior cervicals of *Yunyangosaurus* (*Dai et al., 2020*), whereas all the postaxial cervical vertebrae bear such rim in *Torvosaurus* (*Britt, 1991*). In all postaxial cervicals, the anterior and posterior articular surfaces are slightly wider than high.

The lateral surface of each of the postaxial cervical centra is excavated by a single pleurocoel, which is positioned posterodorsal to the parapophysis. In the third cervical (Fig. 13 A) the pleuroceol deeply invades the lateral surface of the centrum, leading to a very transversely narrow ventral surface (Fig. 14 C) of ~~central part~~. But this narrowing ventral surface does not run through the whole length of centrum to form a ventral keel. The ventral surfaces of following cervical vertebrae become broad and flat and by the 10th cervical vertebra the ventral keel appears with a ventrally vaulted process anterior to it. In the fourth and fifth cervical, the pleuroceol is leading to the neural canal. In the eighth and ninth cervical the pleuroceol is anteroposteriorly elongated and dorsally roofed by a thin lamina.

The diapopysis of each postaxial cervical is lateroventrally extended, and bears a smooth articular surface with ellipse profile. The parapophysis is positioned ventral to the mid-height of the centrum and adjacent to the anterior articular surface in each cervical. In the third and the last two cervicals the parapophysis is strongly shortened and ended with oval-shaped surface, whereas it protrudes lateroventrally in other cervicals. The laterally elongated parapophyses in medial cervicals also occur in *Neovenator* (*Brusatte et al., 2008*). In the last cervical the parapophysis is followed by a prominent ridge, which marks the bottom of the pleurocoel and shallows posteriorly.

The prezygopophysis projects anteriorly from the base of diapophysis, and is connected with the diapophysis laterally through the prezygodiapophyseal lamina (prdl). The paired prezygopophyses are well separated dorsolateral to the neural arch, and are medially connected by the intraprezygopophyseal lamina (tprl). The prezygopophysis has a sub-ellipse shaped and smooth articular facet, which faces anterodorsally and medially. The spinoprezygopophyseal lamina (sprl) laterally demarcates this facet, and connect the prezygopophysis with the neural spine. Throughout the whole cervical series this facet turns more anteromedially, and the anteroposterior distance between pre- and postzygopophysis gradually shortens. The posterodorsally and laterally projected postzygopophysis is more strongly developed than the prezygopophysis, with lateroventrally and posteriorly faced articular surface. In the last three cervicals (Fig. 13 F-H), the postzygopophyseal facets turn to face more posteriorly than that of the preceding elements in the series. The postzygodiapophyseal lamina (podl) runs from the base of the diapophysis posteriorly to the distal end of the postzygopophysis or epipophysis. The spinopostzygopophyseal lamina (spol) originates posteriorly form the base of the neural spine and ends at the distal end of the articular surface of the postzygopophysis. Only the first three postaxial cervicals have well developed epipophysis, which emerges posterolaterally and dorsally to the postzygopophysis. In fourth and fifth cervical the epipophysis is extended well beyond the posterior margin of the postzygopophysis and forms a dorsoventrally thin plate-like structure.

In the third and fourth cervical (Fig. 13 A, B), the anterior rim of the neural spine bears an anterodorsal oriented process, resulting the concave lateral profile above and below this process. Such process positioned at the anterodorsal rim of the anterior cervicals also occurs in *Acrocanthosaurus* (*Harris, 1998*), but in ~~which~~ this process protrudes more anteriorly and past the base of neural spine. The posterior rim of the neural spine of these two elements is posterodorsally convex, thus the posteriormost point is situated at nearly midheight. In subsequent cervicals the neural spine increases in height gradually, and is dorsoventrally higher than anteroposteriorly long since the sixth cervical. In the eighth, ninth and tenth cervicals (Fig. 13 F-H) the neural spine is prominently dorsally elongated, with the distal end fanning out anteroposteriorly in lateral view. ~~Whereas~~ in derived metriacanthosaurids (*Dong et al., 1983*; *Currie & Zhao, 1993*; *Gao, 1992, 1999*), neural spines in posterior cervical vertebrae are slender and rod-like, ~~this condition might provide more spaces for upward mobility of the neck.~~ In ninth (Fig. 14 G-I) and 10^{th} cervicals, a shallow groove runs dorsoventrally along the anterior and posterior rims of the neural spine.

Several bony laminae connect the neural arch and the centrum and separate the space between them into several pneumatic chambers as in most Theropods. In the first five postaxial cervicals the anterior centrodiapophyseal lamina (acdl) and centraprezygopophyseal lamina (cprl) are not very developed and laterally obscured by the ventrally oriented diapophyses. Due to the short distance between the neural arch and centrum in anterior cervicals, the centrapostzygopophyseal laminae of these elements are poorly-developed. In the rest of the cervical series the distance between the arch and centrum increases with the elevation of the diapophysis from the parapophysis, resulting that aforementioned three bony laminae become more prominent. In the first three postaxial cervicals the postzygodiapophyseal laminae (podl) do not continue onto the pedicle of the diapophyses. In the third cervical this lamina is especially weak-developed and even discontinuous to the base of the postzygopophysis. In the last three cervicals, a pneumatic fossa excavates anteriorly into the ventral surface of the postzygodiapophyseal lamina (podl), as in *Sinraptor* (*Currie & Zhao, 1993*). All postaxial cervicals bear notable prezygodiapophyseal laminae (prdl) and posterior centradiapophyseal laminae (pcdl).

The first dorsal vertebra (Fig. 13 I) is platycoelous, with a flat anterior articular surface and a slightly concave posterior articular surface. The anterior and posterior articular surface are slightly wider than high as in cervical vertebrae. The neural arch and the centrum of the first dorsal vertebra are in further distance compared to those in the cervical vertebrae. This extension is followed by the more elongated bony laminae connecting the neural arch and the centrum. The diapophysis is more laterally and horizontally oriented instead of pointing ventrolaterally. The parapophysis does not protrude laterally and its articular surface is immediately lateral to the anterior articular surface of the centrum and subtriangular in shape. The pre- and postzygopophysis decreases in height, followed by the reduction of inclination of the pre- and postzygodiapophyseal lamina in lateral view. The neural spine is approximately 1.5 times as dorsoventrally high as anteroposteriorly long, with a sub-rectangular lateral profile. The groove running along the anterior rim of the neural spine excavates deeper than those of former cervical vertebrae. As in postaxial cervicals, a single pleurocoel penetrates either side of the centrum, but these pelurocoels on both left and right side are straightly connected without any bony walls. The ventral part of the centrum is similar to that of the last cervical vertebra, with a ridge originated from the posterior end of the parapophysis forming the lateral floor of the peurocoel, and a developed ventral keel running through the centrum.

Phylogenetic analysis

The phylogenetic analysis resulted in 1152 MPTs, with each MPTs having a length of 1290 steps (CI = 0.364, RI = 0.660). The strict consensus tree (Fig. 14) places *Yuanmouraptor* at the most 'basal' position in the Metriacanthosauridae, forming a polytomy with *Xuanhanosaurus* and a monophyletic group defined by *Yangchuanosaurus* and *Sinraptor*. The Metriacanthosauridae in our analysis is supported by seven unambiguous synapomorphies: squamosal forms a flange covering quadrate head laterally (character 87-1); acute angle between the occipital condyle and the basal tubera (character 123-1); external mandibular fenestra is 15% longer than the total mandible length (character 133-1); dorsoventral depth of surangular above external mandibular fenestra less than half of the height of mandible (character 134-0); well-developed and broad spinopostzygopophyseal lamina (character 183-0); manus shorter than arm plus forearm (character 268-0); presence of metacarpal IV but lack of IV phalanges and whole digit V (character 269-0). Furthermore, three major lineages of basally branching tetanurans (Megalosauroidea, Coeluerosauria, and Allosauroidea) are supported by this phylogenetic analysis, and recovered a Carnosauria in which Piatnitzkysauridae forms the sister-group to Avetheropoda (Allosauroidea + Coelurosauria).

DISCUSSION

Comparison with Jurassic Metriacanthosauridae in China and morphology transition within Metriacanthosauridae lineage

As shown in the result of our phylogenetic analysis, the metriacanthosaurids excluding *Xuanhanosaurus* (*Dong, 1984*) and *Yuanmouraptor* formed two lineages together to form a monophyletic clade within Metriacanthosauridea. In other words, *Yuanmouraptor*, *Xuanhanosaurus*, and the clade formed a basal trichotomy within Metriacanthosauridae.

The Middle Jurassic *Xuanhanosaurus* (*Dong, 1984*) was considered to fall within Megalosauroidea or in close relationship with Piatnitzkysauridae in previous studies (*Benson, 2010*; *Rauhut et al., 2016*; *Rauhut & Pol, 2019*; *Dai et al., 2020*). In our phylogenetic analysis, *Xuanhanosaurus* was recovered as a member of Metriacanthosauridae, as in *Carrano et al. (2012)*, but this placement is poorly supported with only two characters: relatively short manus and developed metacarpal IV with lack of IV phalanges and digit V, shared with CNM V214 (*Dong et al., 1983*) and *'Szechuanosaurus' zigongensis* (*Gao, 1993*) respectively. Therefore, the phylogenetic position of *Xuanhanosaurus* still needs to be testified by a detailed study of the taxon in the future. The overlapping materials of *Xuanhanosaurus* with *Yuanmouraptor* are limited to two posterior cervical vertebrae. The eighth cervical centrum of *Xuanhanosaurus* is evidently opisthocoelous, in contrast with the platyceolous condition in that of *Yuanmouraptor*. Due to the uncertain phylogenetic position of *Xuanhanosaurus*, *Yuamouraptor* is considered as the most basal representative of Metriacanthosauridae.

Sinraptor dongi (*Currie & Zhao, 1993*), *S. hepingensis* (*Gao, 1992, 1999*), and *Yangchuanosaurus shangyouensis* (*Dong et al., 1978, 1983*) represent derived members in Metriacanthosauridea and all lived in Late Jurassic. Materials of these taxa reach a high degree of completeness, and provide significant taxonomic information. These three taxa are large-sized theropods, and the skull length could reach approximately two times the condition in *Yuanmouraptor*. In *S. dongi*, *S. hepingensis*, and *Y. shangyouensis*, the skull and vertebrae are highly pneumatized, such as the pneumatic foramen on the lateral surface of the jugal and perforated pleurocoels on the axial centrum. ~~Whereas in *Yuanmouraptor* the jugal and axial centrum are not pneumatized.~~ The ventral process of the postorbital of three derived metriacanthosaurids has a small suborbital flange, which might mark the ventral limit of the eyeball, whereas in *Yuanmouraptor* the ventral process of the postorbital is smooth and slightly concave below the eyeball. All three derived metriacanthosaurids bear rugose ornaments on the upper part of the skull, such as heavy rugosity on the nasal, well-developed lacrimal horn, and large rugose boss forming the anterior process of the postorbital. Though the nasal of *Yuanmouraptor* was not preserved, the lacrimal and postorbital only possess slight rugosity. The cervical vertebrae of derived metriacanthosaurids are strongly opisthocoelous with ball and socket articular surface, and the axial intercentrum is anterodorsally flexed. This condition shows greater mobility than that of *Yuanmourpator*, in which the cervical vertebrae are platycoelous and the ventral surface of the axial intercentrum is continuous with that of the centrum. The anteroposteriorly narrow neural spines in posterior cervical vertebrae also indicate a more upward flexible neck in derived metriacanthosaurids. By contrast, the sheet-like neural spines of posterior cervical vertebrae in *Yuanmouraptor* might limit the upward flexibility of the neck.

Within the monophyletic clade excluding *Yuanmouraptor* and *Xuanhanosaurus* in the Metriacanthosauridae, one lineage leads to *Yangchuanosaurus* (*Dong et al., 1978, 1983*), and another lineage is represented by *Sinraptor* (*Gao, 1992*; *Currie & Zhao, 1993*). The clade comprising the members of the latter lineage was named as Metriacanthosaurinae by *Carrano et al. (2012)*. These two lineages are distinct in many aspects. In the axial skeleton, the anterior dorsal vertebrae of Metriacanthosaurinae have prominent ventral keel, whereas in another lineage the keel is weakly developed. In the pelvic girdle, the angle between the long axis of pubis and pubic boot is less than 60° in Metriacanthosaurinae, ~~distinguished from the nearly perpendicular boot and shaft of the pubis in~~ *Yangchuanosaurus* lineage. In Metriacanthosaurinae the ischial shaft is ventrally curved and the distal end is slightly expended, ~~which differs from that~~ the ischial shaft is straight and the distal end of ischium is notably expended to form an ischial boot in

Yangchuanosaurus lineage. ~~Whereas the distal end of the ischium of *Yangchuanosaurs shangyouensis* is slightly expended and similar to the condition in Metriacanthosaurinae~~, might suggesting that this trait is gained independently in these taxa. In the hindlimbs, members of Metriacanthosaurinae possess bulbous fibular crest on the tibia, in contrast to the narrow and lamina-like fibular crest of the tibia in *Yangchuanosaurus* lineage.

Shidaisaurus (*Wu et al., 2009*) was found in Chuanjie Formation (Middle Jurassic) in Lufeng City, Yunnan, which is 85 km from the type locality of *Yuanmouraptor*. *Shidaisaurus* was the first tetanuran reported in Yunnan Province. The skull roof, dorsal part of the occiput, and axis of *Shidaisaurus* are preserved, and these elements could be compared with *Yuanmouraptor*. Both *Yuanmouraptor* and *Shidaisaurus* possess paired frontals broader than long, which generally occur in Allosauroidea; however, in Megalosauroidea and more basal therapods, the paired frontals are anteroposteriorly longer than transversely wide. Similar to *Shidaisaurus*, a slight margin of the frontal contributes to the dorsal margin of the orbit in *Yuanmouraptor*, this also occurs in *Sinraptor dongi* (*Currie & Zhao, 1993*). The supratemporal fossa of *Shidaisaurus* is bounded by abruptly elevated surfaces of the frontals and parietal, which form a very clear border of the supratemporal fossa, this is similar to the condition in *Sinraptor dongi* (*Currie & Zhao, 1993*). Whereas in *Yuanmouraptor*, the border of the supratemporal fenestra does not have well-defined boundary, and the surfaces of the surrounding frontals and parietal are plain and gently sloped. The occiput of *Shidaisaurus* and *Yuanmouraptor* share a similar posteroventrally directed paroccipital process, with the ventral base ~~of which~~ located beneath the occipital condyle, a condition generally developed in Allosauroidea. However, the supraoccipital of *Yuanmouraptor* forms a moderate part of the dorsal rim of the foramen magnum, differing from *Shidaisaurus* in which the supraoccipital does not contribute to form the dorsal margin of the foramen magnum. An atlas-axis complex is the only preserved cervical element of *Shidaisaurus*. The axial centrum of *Shidaisaurus* bears some similarities to that of *Yuanmouraptor*, including broad spinopostzygapophyseal lamina and ~~absence of~~ pleurocoels. The axial intercentrum of *Shidaisaurus* has an anterodorsal inclined ventral surface, followed by an anterodorsally faced anterior articular surface, which resembles the condition in derived metriacanthosaurid *Yangchuanosaurus* (*Dong et al., 1983*) and *Sinraptor* (*Currie & Zhao, 1993*). However, the alignment of the atlas-axis complex is different in *Yuanmouraptor*, in which the ventral surface of the axial intercentrum is parallel with the axial centrum, but the anterior articular surface of the axial intercentrum also faces anterodorsally, resulting in a triangular lateral profile of the axial intercentrum. This indicates that *Yuanmouraptor* could also bring the neck underneath the occipital condyle more or less to support the skull as more derived Late Jurassic metricanthosaurids, and might represent an early stage of the arrangement of the atlas-axis complex during the evolution of Metriacanthosauridae. Although *Yuanmouraptor* and *Shidaisaurus* share similar geological distribution and approximately contemporaneous stratigraphic unit which were known as Middle Jurassic (*Huang et al., 2005*; *Fang et al., 2008*), the difference in morphology along with the ~~support~~ of our phylogenetic analysis ~~shows~~ the validity of *Yuanmouraptor jinshajiangensis* gen. et sp. nov.

The Late Jurassic CNM V214 (*Dong et al., 1983*) and the Middle Jurassic *'Szechuanosaurus' zigongensis* (*Gao, 1992*) are also positioned as derived metriacanthosaurids by the phylogenetic analysis and form a monophyletic group with *Sinraptor dongi* (*Currie & Zhao, 1993*), *Sinrptor hepingensis* (*Gao, 1992*), and *Yangchuanosaurus* (*Dong et al., 1978, 1983*). The first reports of CNM V214 and *'S.' zigongensis* regarded them as the neotype of *'Szechuanosaurus' campi* (*Young, 1942*) and a new species of the genus *'Szechuanosaurus'* respectively. The type species of genus *'Szechuanosaurus'*, *'S. campi'*, was based on four isolated teeth, and was considered as invalid (*Wu et al., 2009*; Carrano et al., 2012). Due to the lack of detailed restudies and phylogenetic analyses of these two specimens for decades, CNM V214 and *'S.' zigongensis* have not been given the formal taxonomic names so far. The information about CNM V214 is very limited, with part of the cervical series overlapping with *Yuanmouraptor*. The axial complex of CNM V214 is similar to that of *S.dongi*, *S. hepingensis*, and *Yangchuanosaurus*, with the anterodorsally tilted ventral surface of the intercentrum and well-developed pleurocoels on the centrum. The maxilla of *'S.' zigongensis* is similar to that of *Yuanmouraptor*, with well-developed antorbital fossa. However, the morphology of the posterior cervical vertebrae of *'S.' zigongensis* resembles the condition in those Late Jurassic forms, in which the neural spines are anteroposteriorly narrow and rod-like.

Many character transitions occurred during the evolution of Metriacanthosauridae from the Middle Jurassic to the Late Jurassic. First, as shown in *Yuanmouraptor*, the basal-branching Middle Jurassic members of this clade do not possess a well-developed pneumatic system as in those Late Jurassic descendants, such as the lack of pneumatic foramen on jugal and pleurocoels on axial centrum. The latter condition also occurs in basal-branching metriacanthosaurid *Shidaisaurus* (*Wu et al., 2009*). Second, the ornamentations of the skull have been changed from a slight rugose brow in *Yuanmouraptor* to a prominent lacrimal horn and heavy rugosity on postorbital in *Sinraptor* (*Gao, 1992*; *Currie & Zhao, 1993*) and *Yangchuanosaurus* (*Dong et al., 1983*). Third, the alignment of the atlas-axis complex and morphology of cervical vertebrae have been changed to improve the mobility of the neck. In the primitive stage, as shown in *Yuanmouraptor*, the ventral surface of the axial intercentrum and centrum are continuous, and subsequent cervical vertebrae are platycoelous. This condition has been changed to that the ventral surface of axial intercentrum is notably inclined anterodorsally to bring the neck underneath the skull and cervical vertebrae are strongly opisthocoelous with ball-and-socket articular surface in *Yangchuanosaurus* and *Sinraptor*. Furthermore, to increase the upward flexibility of the posterior part of the neck, the neural spines of posterior cervical vertebrae altered from sheet-like in *Yuamouraptor* to rod-like in those Late Jurassic descendants. Two Middle Jurassic taxa, *Shidaisaurus* and *'Szechuanosaurus' zigongensis* (*Gao, 1993*) could be regarded as transitional forms. In *'Szechuanosaurus' zigongensis* (*Gao, 1993*), the neural spines of posterior cervical vertebrae are also anteroposteriorly constricted and nearly rod-like, but the articular surfaces of cervical centra are platycoelous. *Shidaisaurus* possesses anterodorsally inclined axial intercentrum, but lacks pleurocoels on the axial centrum.

Implications on phylogeny of basal-branching tetanurans

Since three major lineages (Megalosauroidea, Allosauroidea, and Coelurosauria) within Tetanurae were proposed by *Carrano et al. (2012)*, alternative opinions (*Rauhut & Pol, 2019*; *Lamanna et al., 2020*; *Schade et al., 2023*; *Rauhut et al., 2024*) upon the interrelationship of tetanurans were put forward in past decade. Although the result recovered by our phylogenetic analysis approaches to the three-major-clade pattern within Tetanurae, this topology of diverging is unstable with relatively low scores of Bremer support in many nodes (see the online Supplemental File S2 for details). Among the nodes within Tetanurae, Spinosauridae and Coelurosauria (with the exception of *Lourinhanosaurus*) are well-supported, with Bremer support scored 3. Besides, Allosauria (Allosauridea + Carcharodontosauria), and Metriacanthosaurinae (*Carrano et al., 2012*) are less well supported with Bremer support scored 2. However, the placement of Piatnitzkysauridae within the Allosauroidea is rather stable, with three additional steps needed to recover its affinity to Megalosauroidea. The low Bremer support of many nodes within Tetanurae might suggest that independent acquirements of characters occurred multiple times during Early and Middle Jurassic. At least eight taxa from western China are located near the node Allosauroidea by our phylogenetic analysis, but taxa of other clades of basal tetanurans in this region are scarce, this is probably due to the artificial effects rather than the reflection of real proportion of different clades within basal-branching tetanurans. The finding of *Yuanmouraptor* provides an example of early stage in tetanuran evolution. Many characters present in *Yuanmouraptor* are shared with megalosaurid theropods or non-tetanuran theropods, indicating that high level of similarities among these Early and Middle Jurassic theropods. Thus, findings of key taxa to bridge the gap between non-tetanuran ancestors and a variety of derived tetanuran clades are important to testify whether similar character states in different clades are the result of homology or homoplasy. Meanwhile, the construction and sampling of characters, accuracy of state scores, and issues of sampling are also strongly related to alleviate phylogenetic uncertainty (*Lovegrove et al., 2024*). The review and redescription of the named taxa are of great significance. There are still many taxa (*Dong et al., 1978*; *He, 1984*; *Dong et al., 1983*; *Dong & Tang, 1985*; *Gao, 1992*, *1993*, *1999*; *Li et al., 2009*) reported in China lacking detailed osteological descriptions. New anatomic information helping to resolve the phylogenetic problems will be extracted after the detailed re-examination and description of those taxa in future works.

CONCLUSIONS

A new metriacanthosaurid, *Yuanmouraptor jinshajiangensis* gen. et sp. nov, is established based on a relatively complete skull, a complete cervical series, and an anterior-most dorsal vertebra. *Yuanmouraptor* is diagnosed by a unique combination of characters, especially six autapomorphies. Phylogenetic analysis placed *Yuanmouraptor* at a basal-branching position within Metriancanthosauridae. Although the type locality and living age of *Yuanmouraptor* resemble those of *Shidaisaurus*, many characters manifest that these two are different taxa. *Yuanmouraptor* presents the most complete craniums among basal-branching tetanurans reported in Middle Jurassic China, and provides valuable information concerning the morphology transition of cranium and cervical vertebrae during the cause of metriacanthosaurid evolution. In addition, our phylogenetic analysis recovered that the phylogenetic position of Piatnitzkysauridae is more closed to Allosauroidea than to Megalosauroidea, and three major lineages within Tetanurae are supported. However, due to the lack of consensus upon the phylogenetic relationship within basal-branching tetanurans over past decades, more accuracy in character coding and new findings of early members of this clade are needed to testify this new alternative phylogenetic topology.

INSTITUTIONAL ABBREVIATIONS

CNM Chongqing Natural History Museum;

LFGT The Bureau of Natural Resources of Lufeng City, Yunnan, China.

Acknowledgements

This research greatly benefited from discussions with Qian-Nan Zhang, Ya-Ming Wang, Yan-Chao Wang, and Jian Yi. This research was supported by the National Natural Science Foundation of China (42288201, 42372030, and 42002014), the Beijing Natural Science Foundation (5224037) and Expert Local Level Scientific Workstation of Yunnan Province.

References

Allain R. 2002. Discovery of megalosaur (Dinosauria, Theropoda) in the middle Bathonian of Normandy (France) and its implications for the phylogeny of basal Tetanurae. *Journal of Vertebrate Paleontology* **22(3)**:548-563. DOI 10.1671/0272-4634(2002)022[0548:Domdti]2.0.Co;2

Barker CT, Hone DWE, Naish D, Cau A, Lockwood JAF, Foster B, Clarkin CE, Schneider P, Gostling NJ. 2021. New spinosaurids from the Wessex Formation (Early Cretaceous, UK) and the European origins of Spinosauridae. *Scientific Reports* **11(19340)**:1-15. DOI 10.1038/s41598-021-97870-8

Barker CT, Naish D, Newham E, Katsamenis OL, Dyke G. 2017. Complex neuroanatomy in the rostrum of the Isle of Wight theropod Neovenator salerii. *Scientific Reports* **7(1)**:3749. DOI 10.1038/s41598-017-03671-3

Benson RBJ. 2008. A redescription of *'Megalosaurus' hesperis* (Dinosauria, Theropoda) from the Inferior Oolite (Bajocian, Middle Jurassic) of Dorset, United Kingdom. *Zootaxa* **1931**:57-67. DOI 10.5281/zenodo.184841

Benson RBJ. 2010. A description of *Megalosaurus bucklandii* (Dinosauria: Theropoda) from the Bathonian of the UK and the relationships of Middle Jurassic theropods. *Zoological Journal of the Linnean Society* **158(4)**:882-935. DOI 10.1111/j.1096-3642.2009.00569.x

Bonaparte JF. 1986. Les Dinosaures (Carnosaures, Allosauridés, Sauropodes, Cetiosauridés) du Jurassique Moyen de Cerro Cóndor (Chubut, Argentine). *Annales de Paléontologie* **72**:247-289.

Britt BB. 1991. The theropods of the Dry Mesa Quarry (Morrison Formation), Colorado: with emphasis on the osteology of Torvo saurus tanneri. *Brigham Young University, Geology Studies* **37**:1-72.

Brusatte SL, Benson RBJ, Currie PJ, Zhao XJ. 2010a. The skull of *Monolophosaurus jiangi* (Dinosauria: Theropoda) and its implications for early theropod phylogeny and evolution. *Zoological Journal of the Linnean Society* **158(3)**:573-607. DOI 10.1111/j.1096-3642.2009.00563.x

Brusatte SL, Benson RBJ, Hutt S. 2008. *The osteology of Neovenator salerii (Dinosauria: Theropoda) from the Wealden Group (Barremian) of the Isle of Wight*: Monograph of the Palaeontographical Society.

Brusatte SL, Carr TD, Erickson GM, Bever GS, Norell MA. 2009. A long-snouted, multihorned tyrannosaurid from the Late Cretaceous of Mongolia. *Proceedings of the National Academy of Sciences* **106(41)**:17261-17266. DOI 10.1073/pnas.0906911106

Brusatte SL, Chure DJ, Benson RBJ, Xu X. 2010b. The osteology of *Shaochilong maortuensis*, a carcharodontosaurid (Dinosauria: Theropoda) from the Late Cretaceous of Asia. *Zootaxa* **2334(1)**:1-46. DOI 10.5281/zenodo.193148

Brusatte SL, Sereno PC. 2007. A new species of *Carcharodontosaurus* (Dinosauria: Theropoda) from the Cenomanian of Niger and a revision of the genus. *Journal of Vertebrate Paleontology* **27(4)**:902-916. DOI 10.1671/0272-4634(2007)27[902:ANSOCD]2.0.CO;2

Brusatte SL, Sereno PC. 2008. Phylogeny of Allosauroidea (Dinosauria: Theropoda): Comparative analysis and resolution. *Journal of Systematic Palaeontology* **6(2)**:155-182. DOI 10.1017/s1477201907002404

Buffetaut E, Suteethorn V, Tong H. 1996. The earliest known tyrannosaur from the Lower Cretaceous of Thailand. *Nature* **381(6584)**:689-691. DOI 10.1038/381689a0

Carr TD, Varricchio DJ, Sedlmayr JC, Roberts EM, Moore JR. 2017. A new tyrannosaur with evidence for anagenesis and crocodile-like facial sensory system. *Scientific Reports* **7(1)**:44942. DOI 10.1038/srep44942

Carrano MT, Benson RBJ, Sampson SD. 2012. The phylogeny of Tetanurae (Dinosauria: Theropoda). *Journal of Systematic Palaeontology* **10(2)**:211-300. DOI 10.1080/14772019.2011.630927

Carrano MT, Loewen MA, Sertich JWJ. 2011. *New materials of Masiakasaurus knopfleri Sampson, Carrano, and Forster, 2001, and Implications for the Morphology of the Noasauridae (Theropoda: Ceratosauria)*: Smithsonian Institution Scholarly Press.

Choiniere JN, Clark JM, Forster CA, Xu X. 2010. A basal coelurosaur (Dinosauria: Theropoda) from the Late Jurassic (Oxfordian) of the Shishugou Formation in Wucaiwan, People's Republic of China. *Journal of Vertebrate Paleontology* **30(6)**:1773-1796. DOI 10.1080/02724634.2010.520779

Colbert EH. 1989. *The Triassic dinosaur Coelophysis*. Arizona: Museum of Northern Arizona Press.

Coria RA, Currie PJ. 2002. The braincase of *Giganotosaurus carolinii* (Dinosauria: Theropoda) from the Upper

Cretaceous of Argentina. *Journal of Vertebrate Paleontology* **22(4)**:802-811. DOI 10.1671/0272-4634(2002)022[0802:Tbogcd]2.0.Co;2

Coria RA, Currie PJ. 2006. A new carcharodontosaurid (Dinosauria, Theropoda) from the Upper Cretaceous of Argentina. *Geodiversitas* **28(1)**:71-118.

Coria RA, Currie PJ. 2016. A New Megaraptoran Dinosaur (Dinosauria, Theropoda, Megaraptoridae) from the Late Cretaceous of Patagonia. *PLoS One* **11(7)**:e0157973. DOI 10.1371/journal.pone.0157973

Coria RA, Salgado L. 1995. A new giant carnivorous dinosaur from the Cretaceous of Patagonia. *Nature* **337**:224-226. DOI 10.1038/377224a0

Cullen TM, Larson DW, Witton MP, Scott D, Maho T, Brink KS, Evans DC, Reisz R. 2023. Theropod dinosaur facial reconstruction and the importance of soft tissues in paleobiology. *Science* **379(6639)**:1348-1352. DOI 10.1126/science.abo7877

Currie PJ, Carpenter K. 2000. A new specimen of *Acrocanthosaurus atokensis* (Theropoda, Dinosauria) from the Lower Cretaceous Antlers Formation (Lower Cretaceous, Aptian) of Oklahoma, USA. *Geodiversitas* **22(2)**:207-246.

Currie PJ, Zhao XJ. 1993. A new carnosaur (Dinosauria, Theropoda) from the Jurassic of Xinjiang, People's Republic of China. *Canadian Journal of Earth Sciences* **30(10)**:2037–2081. DOI 10.1139/e93-179

Dai H, Benson R, Hu XF, Ma QY, Tan C, Li N, Xiao M, Hu HQ, Zhou YX, Wei ZY, Zhang F, Jiang S, Li DQ, Peng GZ, Yu YL, Xu X. 2020. A new possible megalosauroid theropod from the Middle Jurassic Xintiangou Formation of Chongqing, People's Republic of China and its implication for early tetanuran evolution. *Sci Rep* **10(1)**:139. DOI 10.1038/s41598-019-56959-x

Dong ZM. 1984. A new Theropod dinosaur from the middle Jurassic of Sichuan Basin. *Vertebrata Palasiatica* **22(3)**:213-218.

Dong ZM, Tang ZL. 1985. A new Mid-Jurassic theropod (*Gasosaurus constructus* gen et sp. nov.) from Dashanpu, Zigong, Sichuan Province, China. *Vertebrata Palasiatica* **23(1)**:77-83.

Dong ZM, Zhang YH, Li XM, Zhou SW. 1978. A new carnosaur from Yongchuan County, Sichuan Province. *Chinese Science Bulletin* **23(5)**:302-304.

Dong ZM, Zhou SW, Zhang YH. 1983. Dinosaurs from the Jurassic of Sichuan. *Palaeontologica Sinica* **162C(23)**:1-136.

Eddy DR, Clarke JA. 2011. New information on the cranial anatomy of *Acrocanthosaurus atokensis* and its implications for the phylogeny of Allosauroidea (Dinosauria: Theropoda). *PLoS One* **6(3)**:e17932. DOI 10.1371/journal.pone.0017932

Fang XS, Li PX, Zhang ZJ, Cheng ZW, Pang QQ, Zhang ZW, Huang BC. 2008. *The Jurassic Red Bed in the Cental Yunan of China*. Peijing: Geology Press.

Gao YH. 1992. *Yangchuanosaurus hepingensis*-a new species of carnosaur from Zigong, Sichuan. *Vertebrata Palasiatica* **30(4)**:313-324.

Gao YH. 1993. A new species of *Szechuanosaurus* from the middle Jurassic of Dshanpu, Zigong, Sichuan. *Vertebrata Palasiatica* **31(4)**:308-314.

Gao YH. 1999. *A complete Carnosaur skeleton from Zigong, Sichuan: Yangchunosaurus hepingensis*: Sichuan Scientific & Technological Press.

Gauthier J. 1986. Saurischian monophyly and the origin of birds. *Memoirs of the California Academy of Science* **8**:1-55.

Goloboff PA, Morales ME. 2023. TNT version 1.6, with a graphical interface for MacOS and Linux, including new routines in parallel. *Cladistics* **39(2)**:144-153. DOI 10.1111/cla.12524

Harris JD. 1998. *A reanalysis of Acrocanthosaurus atokensis, its phylogenetic status, and paleobiogeographic implications, based on a new specimen from Texas*: New Mexico Museum of Natural History.

He XL. 1984. *The Vertebrate Fossils of Sichuan*. Chengdu: Sichuan Scientific and Technological Publishing House.

Hendrickx C, Hartman SA, Mateus O. 2015. An overview of non-avian therapod discoveries and classification. *PalArch's Journal of Vertebrate Palaeontology* **12(1)**:1-73.

Hendrickx C, Mateus O. 2014. *Torvosaurus gurneyi* n. sp., the Largest Terrestrial Predator from Europe, and a Proposed Terminology of the Maxilla Anatomy in Nonavian Theropods. *PLoS One* **9(3)**:1-25. DOI 10.1371/journal.pone.0088905

Holtz TRJ, Molnar RE, Currie PJ. 2004. Basal Tetanurae. In: Weishampel DB, Dodson P, Osmólska H, eds. *The Dinosauria Second edition*: University of California Press, Berkeley., 71-110.

Huang BC. 2005. Magnetostratigraphy of the Jurassic in Lufeng, central Yunnan. *Geological Bulletin of China* **24(4)**:322-328.

Huene FV. 1923. Carnivorous Saurischia in Europe Since the Triassic. *Geological Society of America Bulletin* **34(3)**:449-458. DOI 10.1130/gsab-34-449

Lamanna MC, Casal GA, Martínez RDF, Ibiricu LM. 2020. Megaraptorid (Theropoda: Tetanurae) Partial Skeletons from the Upper Cretaceous Bajo Barreal Formation of Central Patagonia, Argentina: Implications for the Evolution of Large Body Size in Gondwanan Megaraptorans. *Annals of Carnegie Museum* **86(3)**:255-294. DOI 10.2992/007.086.0302

Li F, Peng GZ, Ye Y, Jiang S, Huang DX. 2009. A new carnosaur from the Late Jurassic of Qianwei, Sichuan, China. *Acta Geologica Sinica* **83(9)**:1203-1213.

Lovegrove J, Upchurch P, Barrett PM. 2024. Untangling the tree or unravelling the consensus? Recent developments in the quest to resolve the broad-scale relationships within Dinosauria. *Journal of Systematic Palaeontology* **22(1)**:234533. DOI 10.1080/14772019.2024.2345333

Lü JC, Li SX, Ji Q, Wang GF, Zhang JH, Dong ZM. 2006. New Eusauropod Dinosaur from Yuanmou of Yunnan Province, China. *Acta Geologica Sinica* **80(1)**:1-10. DOI 10.1111/j.1755-6724.2006.tb00788.x

Lü JC, Li TG, Zhong SM, Ji Q, Li SX. 2008. A New Mamenchisaurid Dinosaur from the Middle Jurassic of Yuanmou, Yunnan Province, China. *Acta Geologica Sinica* **82(1)**:17-26. DOI 10.1111/j.1755-6724.2008.tb00320.x

Madsen JH. 1976a. *Allosaurus fragilis*: a revised osteology. *Utah Geological and Mineral Survey Bulletin* **109(163)**.

Madsen JH. 1976b. A second new theropod dinosaur from the Late Jurassic of east central Utah. *Utah Geology* **3(1)**:51-60.

Madsen JH, Welles SP. 2000. *Ceratosaurus (Dinosauria, Theropoda) a revised osteology*: Utah Geological Survey, Miscellaneous Publications 00-2.

Marsh AD, Rowe TB. 2020. A comprehensive anatomical and phylogenetic evaluation of *Dilophosaurus wetherilli* (Dinosauria, Theropoda) with descriptions of new specimens from the Kayenta Formation of northern Arizona. *Journal of Paleontology* **94(S78)**:1-103. DOI 10.1017/jpa.2020.14

Marsh OC. 1881. Classification of the Dinosauria. *American Journal of Sciences* **23**:81-86.

O'Connor PM. 2007. The Postcranial Axial Skeleton of *Majungasaurus crenatissimus* (Theropoda: Abelisauridae) from the Late Cretaceous of Madagascar. *Journal of Vertebrate Paleontology* **27(sup2)**:127-163. DOI

10.1671/0272-4634(2007)27[127:Tpasom]2.0.Co;2

Owen R. 1842. Report on British Fossil Reptiles, Part. II. Report of the eleventh meeting of the British Association for the dvancement of Science, Held at Plymouth in July 1841.

Paul GS. 1988. Eustreptospondylids and Metriacanthosaurs. In: Cohen IB, Coles R, Dyson F, Feinberg G, Florman SC, Judson HF, Pagels HR, Pollack RE, Seitz F, Zuckerman H, eds. *Predatory Dinosaurs of the World*. New York: Simon & Schuster, 286-293.

Pol D, Rauhut OWM. 2012. A Middle Jurassic abelisaurid from Patagonia and the early diversification of theropod dinosaurs. *Proc Biol Sci* **279(1741)**:3170-3175. DOI 10.1098/rspb.2012.0660

Rauhut OWM. 2004. Braincase structure of the Middle Jurassic theropod dinosaur *Piatnitzkysaurus*. *Canadian Journal of Earth Sciences* **41(9)**:1109-1122. DOI 10.1139/e04-053

Rauhut OWM, Bakirov AA, Wings O, Fernandes AE, Hübner TR. 2024. A new theropod dinosaur from the Callovian Balabansai Formation of Kyrgyzstan. *Zoological Journal of the Linnean Society* **201(4)**:1-51. DOI 10.1093/zoolinnean/zlae090

Rauhut OWM, Hübner TR, Lanser KP. 2016. A new megalosaurid theropod dinosaur from the late Middle Jurassic (Callovian) of north-western Germany: Implications for theropod evolution and faunal turnover in the Jurassic. *Palaeontologia Electronica* **19.2(26A)**:1-65. DOI 10.26879/654

Rauhut OWM, Pol D. 2019. Probable basal allosauroid from the early Middle Jurassic Canadon Asfalto Formation of Argentina highlights phylogenetic uncertainty in tetanuran theropod dinosaurs. *Sci Rep* **9(1)**:18826. DOI 10.1038/s41598-019-53672-7

Sadleir R, Barrett PM, Powell HP. 2008. *The Anatomy and Systematics of Eustreptospondylus Oxoniensis, A Theropod Dinosaur from the Middle Jurassic of Oxfordshire, England*: Monographs of the Palaeontographical Society.

Sampson SD, Witmer LM. 2007. Craniofacial Anatomy of *Majungasaurus crenatissimus* (Theropoda: Abelisauridae) from the Late Cretaceous of Madagascar. *Journal of Vertebrate Paleontology* **27(sup2)**:32-104. DOI 10.1671/0272-4634(2007)27[32:CAOMCT]2.0.CO;2

Schade M, Rauhut OWM, Foth C, Moleman O, Evers SW. 2023. A reappraisal of the cranial and mandibular osteology of the spinosaurid *Irritator challengeri* (Dinosauria: Theropoda). *Palaeontologia Electronica* **26(2)**:1-116. DOI 10.26879/1242

Sereno PC, Beck AL, Dutheil DB, Gado B, Larsson HCE, Lyon GH, Marcot JD, Rauhut OWM, Sadleir RW, Sidor CA, Varricchio DD, Wilson GP, Wilson JA. 1998. A Long-Snouted Predatory Dinosaur from Africa and the Evolution of Spinosaurids. *Science* **282(5392)**:1298-1302. DOI 10.1126/science.282.5392.1298

Sereno PC, Brusatte SL. 2008. Basal Abelisaurid and Carcharodontosaurid Theropods from the Lower Cretaceous Elrhaz Formation of Niger. *Acta Palaeontologica Polonica* **53(1)**:15-46. DOI 10.4202/app.2008.0102

Sereno PC, Dutheil DB, larochene M, Larsson HCE, Lyon GH, Magwene PM, Sidor CA, Varricchio DJ, Wilson JA. 1996. Predatory Dinosaurs from the Sahara and Late Cretaceous Faunal Differentiation. *Science* **272(5264)**:986-991. DOI 10.1126/science.272.5264.986

Sereno PC, Wilson JA, Larsson HCE, Dutheil DB, Sues HD. 1994. Early Cretaceous Dinosaurs from the Sahara. *Science* **266(5183)**:267-271. DOI 10.1126/science.266.5183.267

Smith ND, Makovicky PJ, Hammer WR, Currie PJ. 2007. Osteology of *Cryolophosaurus ellioti* (Dinosauria: Theropoda) from the Early Jurassic of Antarctica and implications for early theropod evolution. *Zoological Journal of the Linnean Society* **151(2)**:377-421. DOI 10.1111/j.1096-3642.2007.00325.x

Walker AD. 1964. Triassic reptiles from the Elgin Area: *Ornithosuchus* and the origin of Carnosaurs. *Philosophical Transactions of the Royal Society of London Series B, Biological Sciences* **248(744)**:53-134.

Wilson JA. 1999. A nomenclature for vertebral laminae in sauropods and other saurischian dinosaurs. *Journal of Vertebrate Paleontology* **19(4)**:639-653. DOI 10.1080/02724634.1999.10011178

Witmer LM. 1997. The Evolution of the Antorbital Cavity of Archosaurs: A Study in Soft-Tissue Reconstruction in the Fossil Record with an Analysis of the Function of Pneumaticity. *Journal of Vertebrate Paleontology* **17(sup001)**:1-76. DOI 10.1080/02724634.1997.10011027

Wu XC, Currie PJ, Dong ZM, Pan SG, Wang T. 2009. A new theropod Dinosaur from the middle Jurassic of Lufeng, Yunnan, China. *Acta Geologica Sinica* **83(1)**:9-24. DOI 10.1111/j.1755-6724.2009.00002.x

Xing LD, Miyashita T, Currie PJ, You HL, Zhang JP, Dong ZM. 2013. A new basal eusauropod from the Middle Jurassic of Yunnan, China, and faunal compositions and transitions of Asian sauropodomorph dinosaurs. *Acta Palaeontologica Polonica* **60(1)**:145-154. DOI 10.4202/app.2012.0151

Xu X, Clark JM, Forster CA, Norell MA, Erickson GM, Eberth DA, Jia CK, Zhao Q. 2006. A basal tyrannosauroid dinosaur from the Late Jurassic of China. *Nature* **439(7077)**:715-718. DOI 10.1038/nature04511

You HL, Azuma Y, Wang T, Wang YM, Dong ZM. 2014. The first well-preserved coelophysoid theropod dinosaur from Asia. *Zootaxa* **3873(3)**:233-249. 10.11646/zootaxa.3873.3.3

Young CC. 1942. Fossil vertebrates from Kuangyuan, N. Szechuan (Sichuan), China. *Bulletin of the Geological Society of China* **22(3-4)**:293-309.

Yu YL, Yi HY, Wang SY, Pei R, Zhang C, Xu X. 2023. A Jurassic Tibetan theropod tooth reveals dental convergency and its implication for identifying fragmentary fossils. *The Innovation Geoscience* **1(3)**. DOI 10.59717/j.xinn-geo.2023.100040

Zhao XJ, Benson RBJ, Brusatte SL, Currie PJ. 2009. The postcranial skeleton of *Monolophosaurus jiangi* (Dinosauria: Theropoda) from the Middle Jurassic of Xinjiang, China, and a review of Middle Jurassic Chinese theropods. *Geological Magazine* **147(1)**:13-27. DOI 10.1017/s0016756809990240

Zhao XJ, Currie PJ. 1993. A large crested theropod from the Jurassic of Xinjiang, People's Republic of China. *Canadian Journal of Earth Sciences* **30(10)**:2027-2036. DOI 10.1139/e93-178

Figure 1

Geographical distribution of metriacanthosaurid theropods in Yunnan, Sichuan, and Chongqing, China.

Each number indicates an individual: 1, *Shidaisaurus jinae*; 2, '*Szechuanosaurus*' *zigongensis*; 3, CNM V214; 4, *Sinraptor hepingensis*; 5 & 6, *Yangchuanosaurus shangyouensis*.

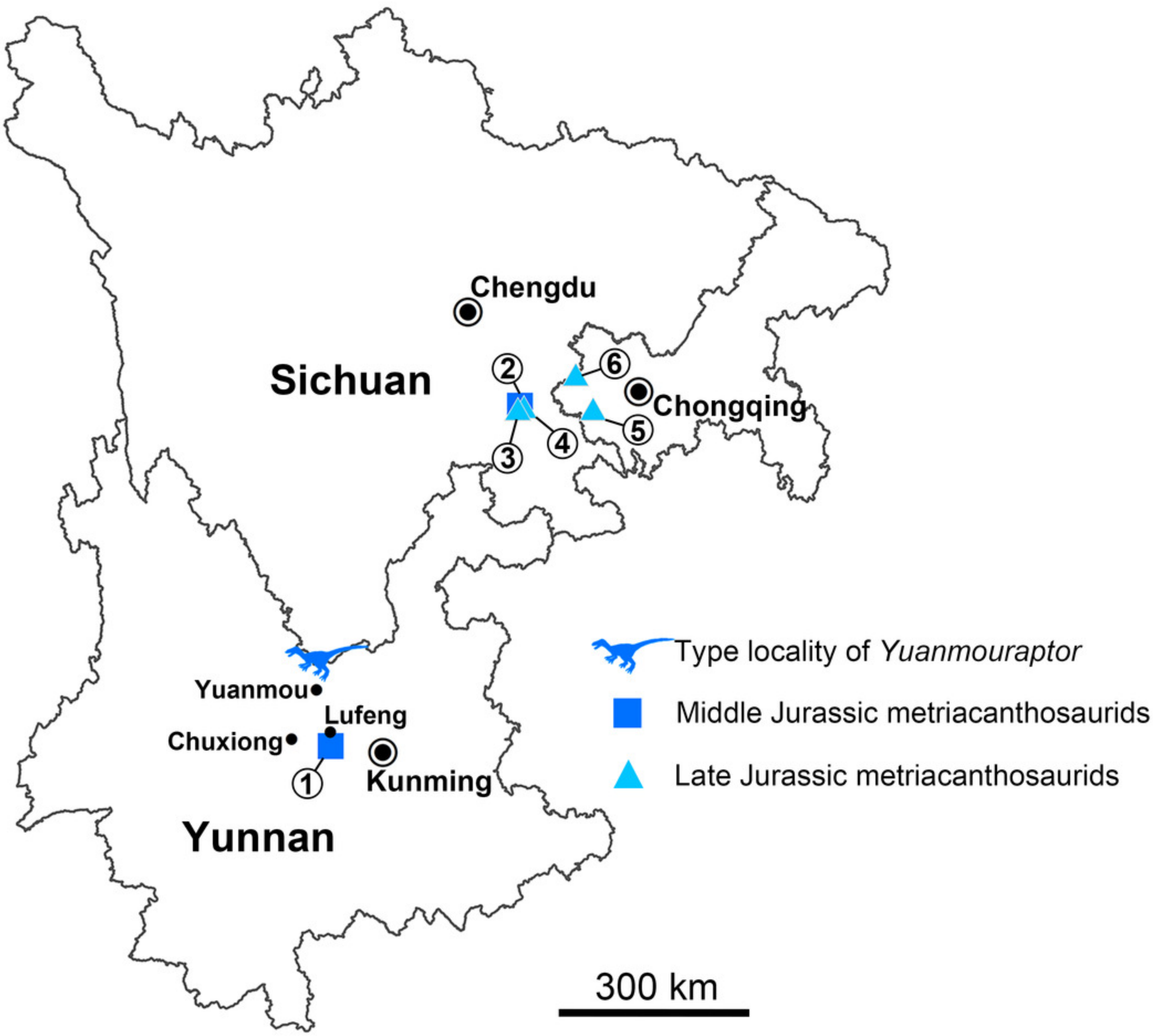

Figure 2

Cranium of *Yuanmouraptor jinshajiangensis* gen. et sp. nov. (LFGT-ZLJ0015).

Cranium in (A) left lateral view with (B) labeled drawing and (C) right lateral view with (D) labeled drawing. Abbreviations: an, angular; ar, articular; bs, basisphenoid; d, dentary; f, frontal, j, jugal; l, lacrimal; lsp; laterosphenoid; m, maxilla; n, nasal; ot, otoccipital; prm, premaxilla; pa, parietal; par, prearticular; pl, palatine; po, postorbital; pop, paroccipital process; pr, prootic; prf, prefrontal; q, quadrate; qj, quadratojugal; sa, surangular; sp, splenial; so, supraoccipital; sq, squamosal. Striated area indicates damage and grey area indicates matrix. Scale bar represents 100 mm. Photos by Xiao-Chun Wu.

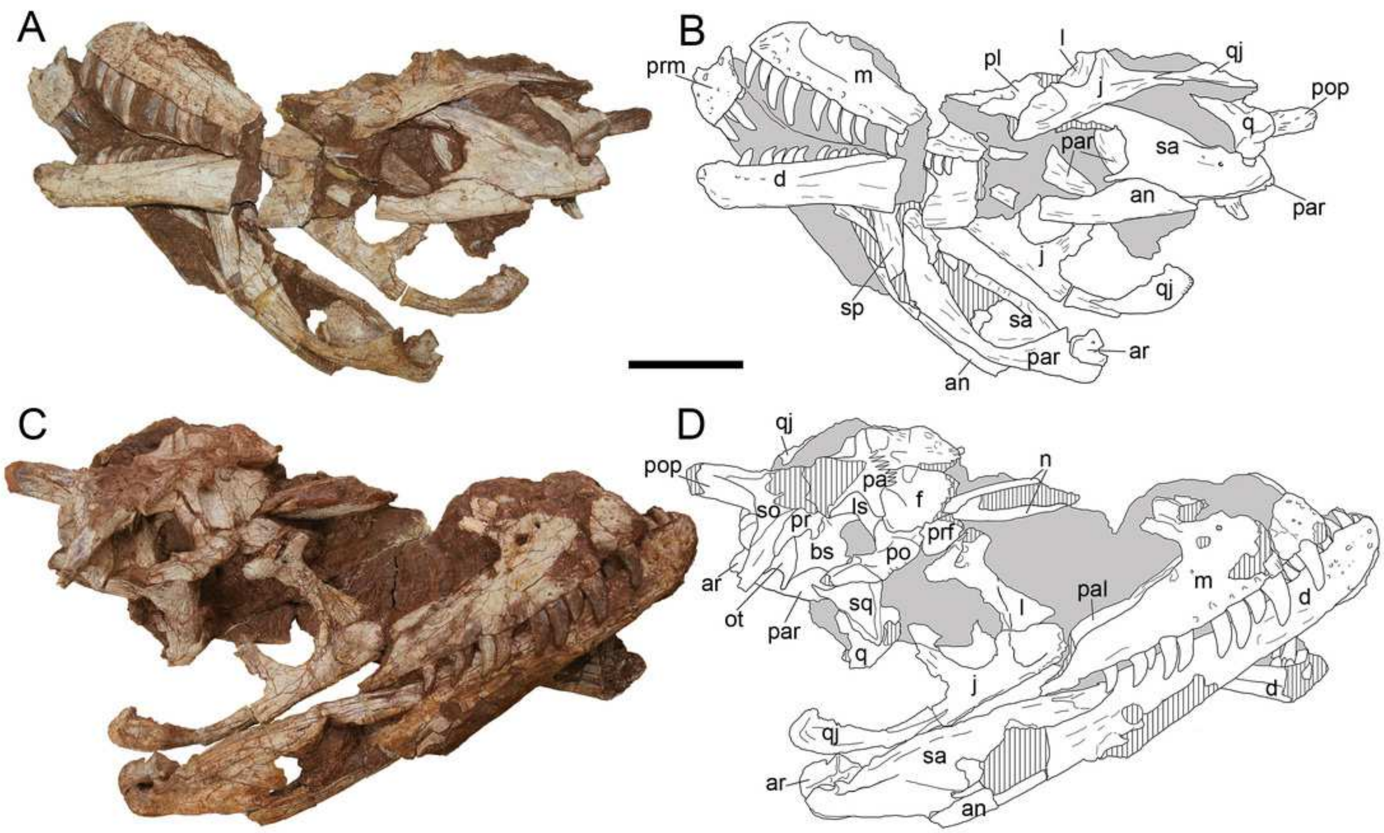

Figure 3

Reconstruction of the cranium of *Yuanmouraptor jinshajiangensis* gen. et sp. nov. (LFGT-ZLJ0015).

Abbreviations: an, angular; bs, basisphenoid; d, dentary; emf, external mandibular fenestra; j, jugal; l, lacrimal; m, maxilla; ot, otoccipital; prm, premaxilla; par, prearticular; pl, palatine; po, postorbital; pop, paroccipital process; pr, prootic; prf, prefrontal; q, quadrate; qj, quadratojugal; sa, surangular; sq, squamosal. Shaded area indicates the missing part, and dashed line marks the margin of breakage of bone. Scale bar represents 100 mm.

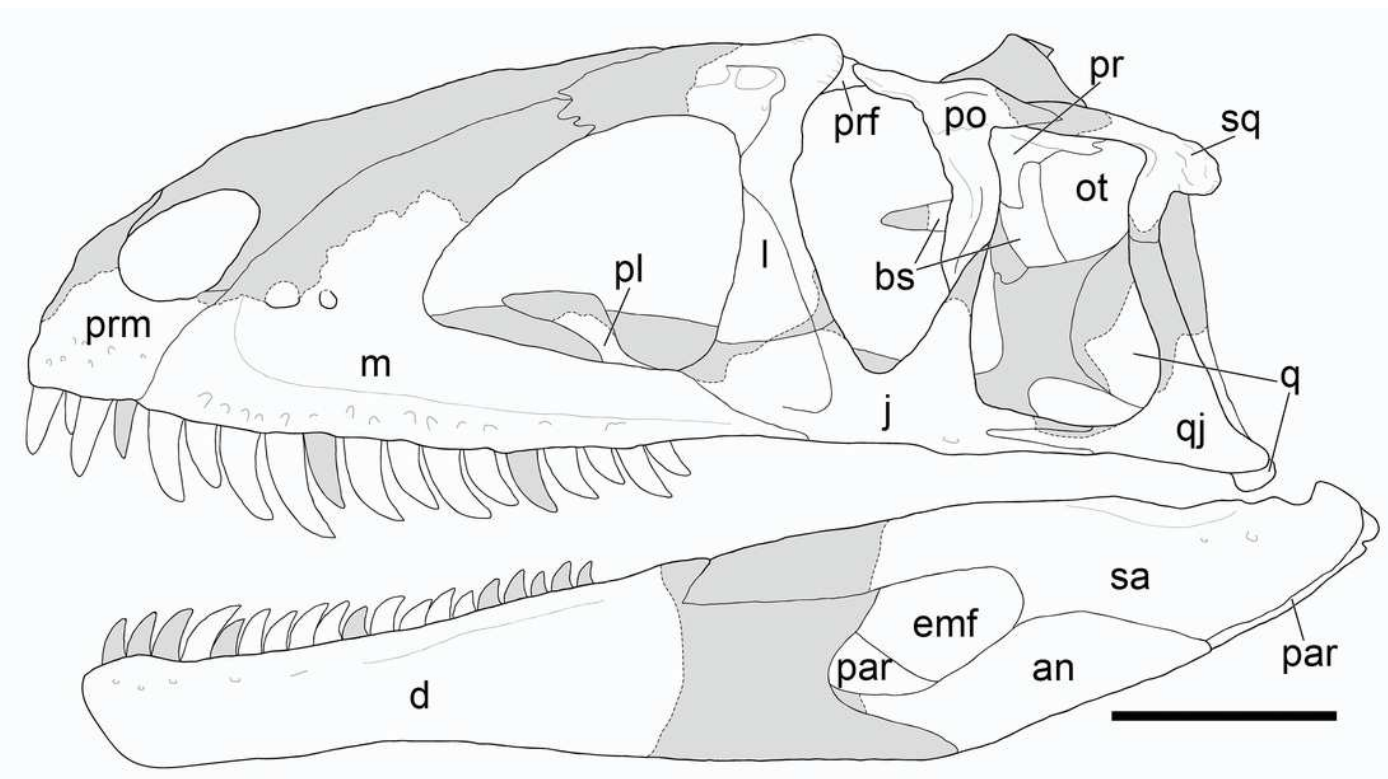

Figure 4

Premaxilla and maxilla of *Yuanmouraptor jinshajiangensis* gen. et sp. nov. (LFGT-ZLJ0015).

Left premaxilla in (A) lateral view with (B) labeled drawing. (C) Serration on the premaxillary teeth, with mesial carina pointed by white arrows. (D) Serration on the mesial and distal carina of the maxillary teeth. Left maxilla in (E) lateral view with (F) labeled drawing. Right maxilla in (G) lateral view with (H) labeled drawing. Abbreviations: aof, antorbital fossa; aofe, antorbital fenestra; asr, remnant ascending ramus of maxilla; en, external naris; mc, maxillary contact; mf, maxillary fenestra; m1-14, maxillary teeth 1-14; nf, narial fossa; np, nasal process; pmf, promaxillary fenestra; prc, premaxillary contact. p1-3, premaxillary teeth 1-3; sn, subnarial process. Striated area indicates damage. Scale bars for A-B present 50 mm, for C-D, 5 mm, and for E-H, 100 mm. Photos by Xiao-Chun Wu and Yi Zou.

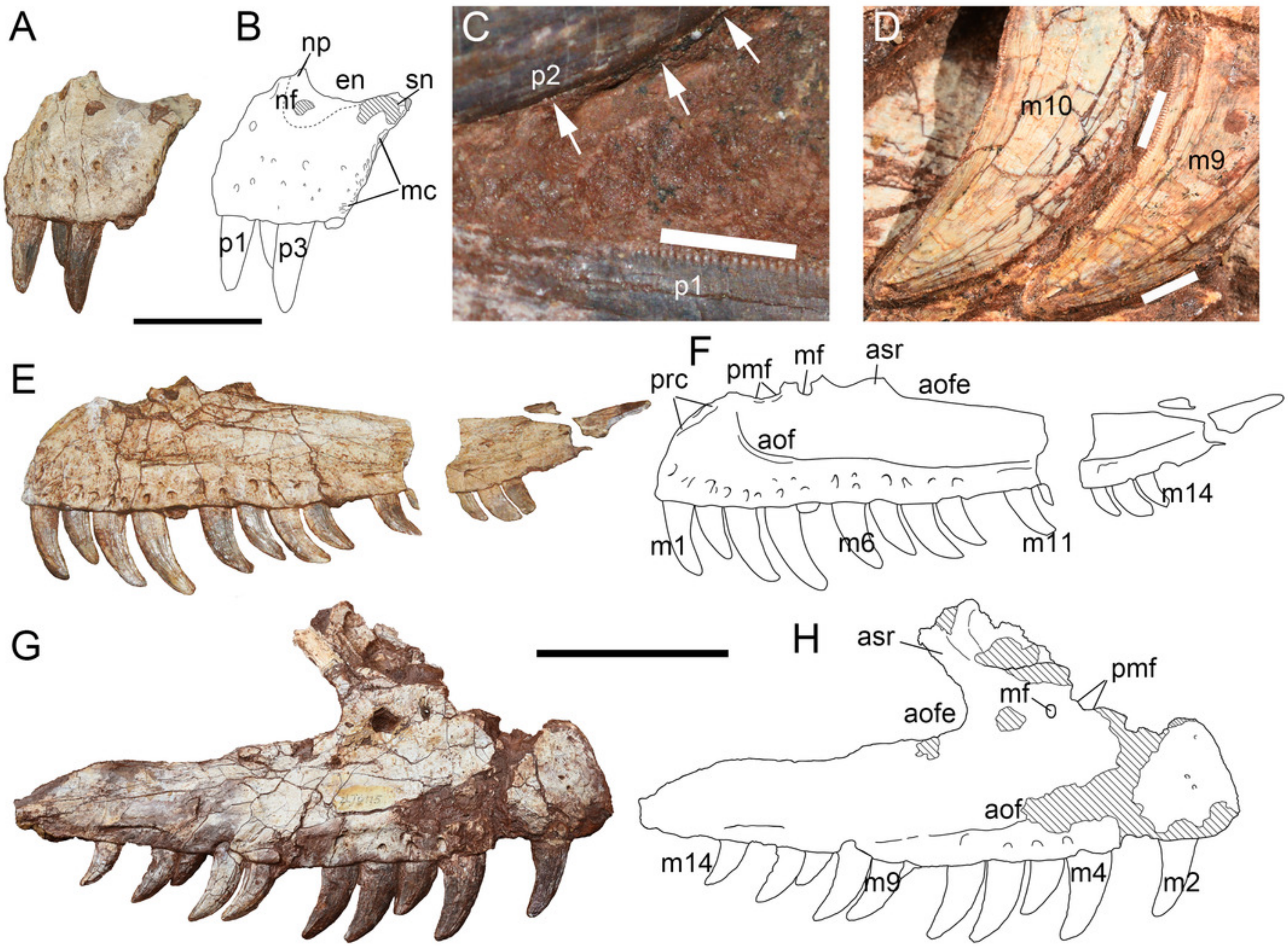
A
B
np
en
sn
nf
mc
p1
p3
C
p2
p1
D
m10
m9
E
F
prc
pmf
mf
asr
aofe
aof
m1
m6
m11
m14
G
H
asr
pmf
mf
aofe
aof
m14
m9
m4
m2

Figure 5

Skull elements of *Yuanmouraptor jinshajiangensis* gen. et sp. nov. (LFGT-ZLJ0015).

Right lacrimal in (A) lateral view with (B) labeled drawing. Articulated right jugal and quadratojugal in (C) lateral view with (D) labeled drawing. Articulated right jugal and quadratojugal in (E) medial view with (F) labeled drawing. Left jugal in (G) lateral view with (H) labeled drawing. (I) Left quadratojugal and partial quadratojugal ramus of left jugal. Abbreviations: aof, antorbital fossa; de, depression; f, flange; fo, fossa; j, jugal; lc, lacrimal contact; lla, lateral lamina; ltf, lateral temporal fenestra; mla, medial lamina; o, orbit; pn, pneumatic foramen; por, postorbital ramus of jugal; qj, quadratojugal; qjr, quadratojugal ramus of jugal. Striated areas indicate damage. Scale bars present 50 mm. Photos by Xiao-Chun Wu and Yi Zou.

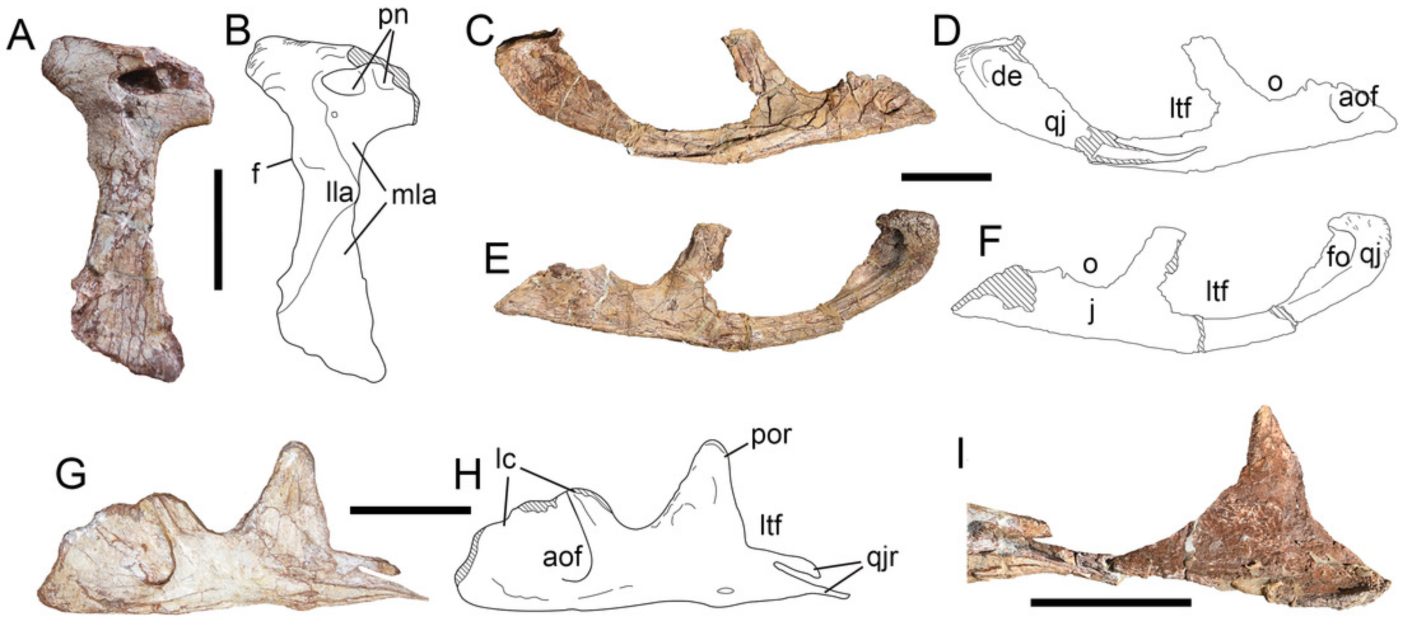

Figure 6

Postorbital and skull roof of *Yuanmouraptor jinshajiangensis* gen. et sp. nov. (LFGT-ZLJ0015)

Right postorbital in (A) lateral view with (B) labeled drawing, and in (C) posterior view with (D) labeled drawing. Skull roof in (E) dorsal view with (F) labeled drawing. Abbreviations: de, depression; f, frontal; l, lacrimal; la, lamina; lsp, laterosphenoid; n, nasal; or, orbital ramus; ot, otoccipital; pa, parietal; po, postorbital; pop, paroccipital process; por, posterior ramus; pr, prootic; prf, prefrontal; r, ridge; so, supraoccipital; stf, supratemporal fenestra; stfo, supratemporal fossa; t, trough; vr, ventral ramus of postorbital. Striated area indicates damage and grey area indicates matrix. Scale bars present 50 mm. Photos by Xiao-Chun Wu.

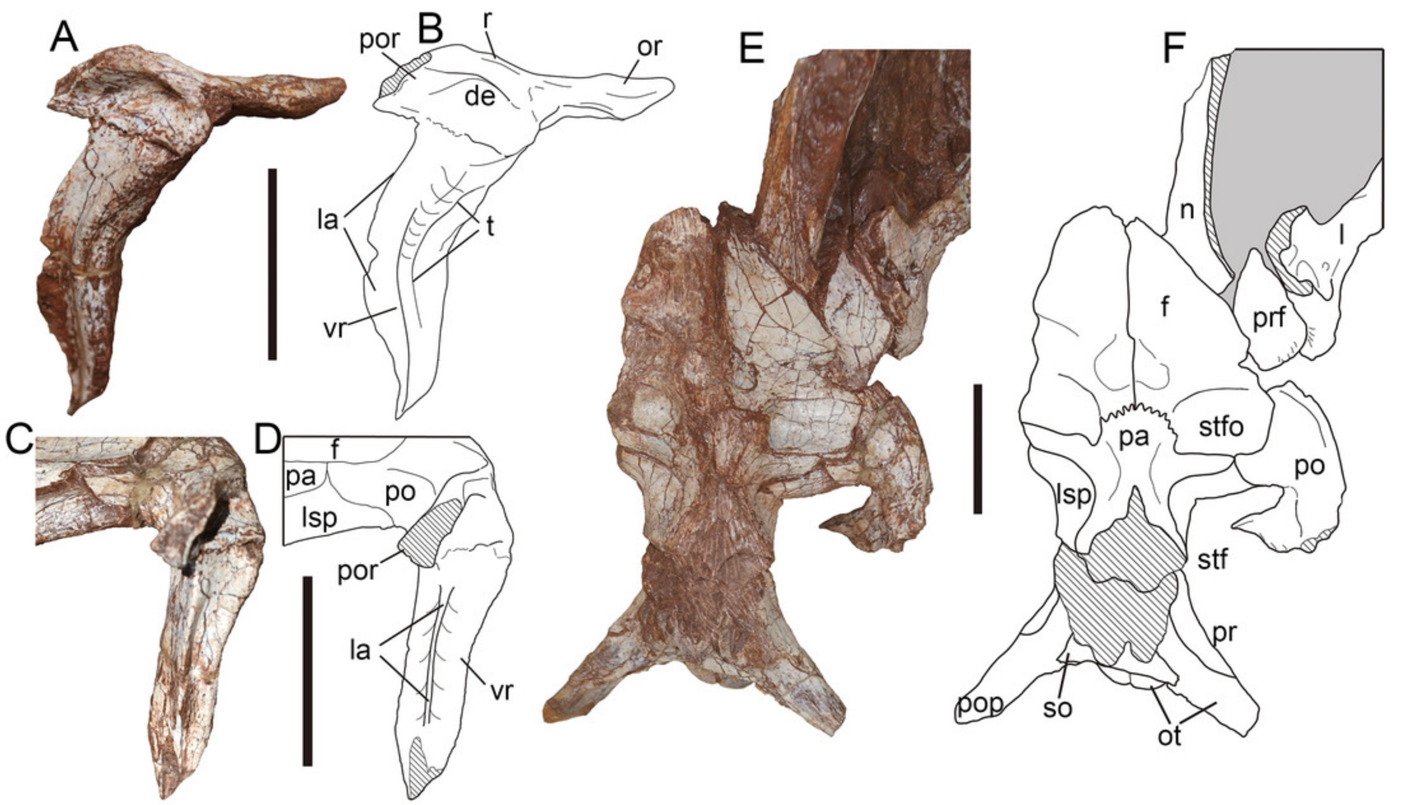

Figure 7

Skull elements of *Yuanmouraptor jinshajiangensis* gen. et sp. nov. (LFGT-ZLJ0015).

Right squamosal in (A) dorsal view with (B) labeled drawing, in (C) posterodorsal view with (D) labeled drawing, and in (E) lateral view. Left quadrate in (F) anterolateral, (G) posterolateral, and (H) ventral views. Left palatine in (I) lateral view with (J) labeled drawing. Abbreviations: ap, anterior process; ecc, ectocondyle; enc, entocondyle; ics, intercondylar sulcus; in, internal naris; ltf, lateral temporal fenestra; mp, medial process; map, maxillary process; pac, parietal contact; po, postorbital; popc, paroccipital process contact; pn, pneumatic foramen; pp, posterior process; qc, contact for quadrate; qs, quadrate shaft; r, ridge; vp, ventral process; vptp, vomeropterygoid process. Striated area indicates damage and grey area indicates matrix. Scale bar presents 50 mm. Photos by Xiao-Chun Wu and Yi Zou.

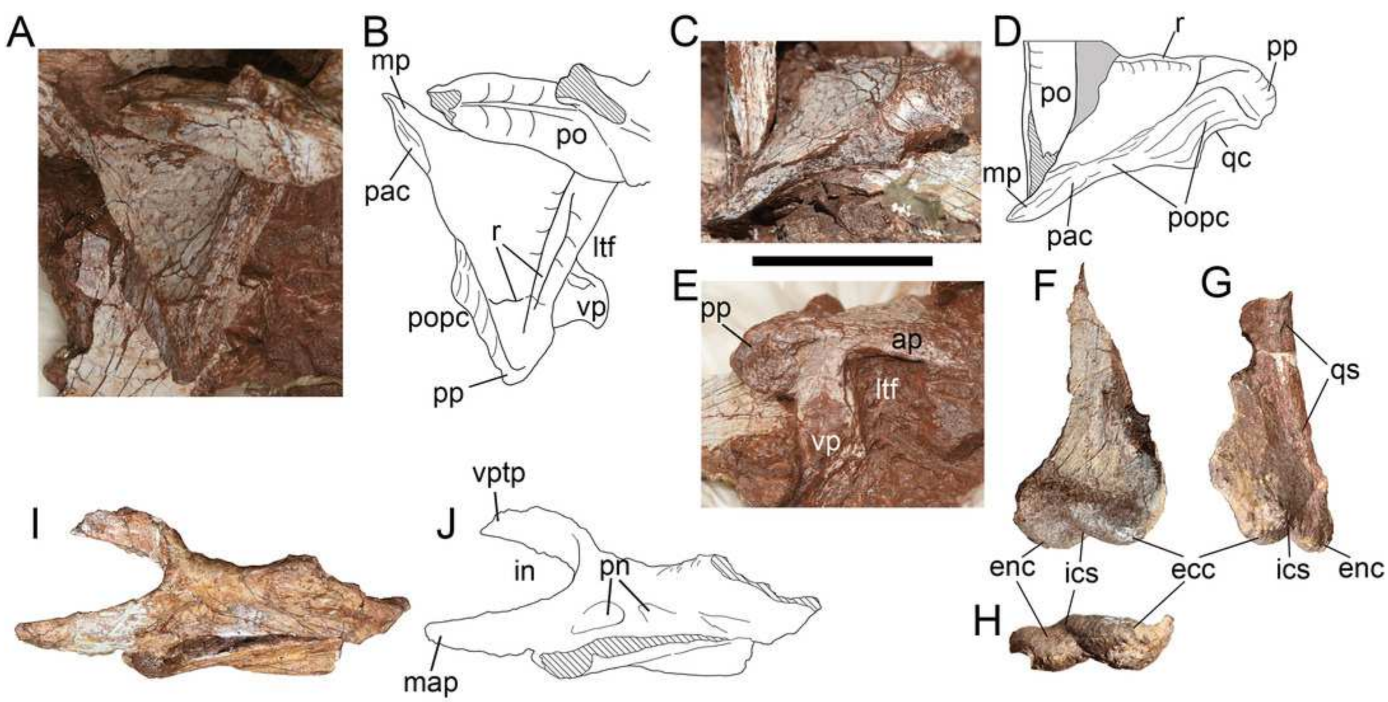

Figure 8

Occiput of *Yuanmouraptor jinshajiangensis* gen. et sp. nov. (LFGT-ZLJ0015).

Supraoccipital and adjacent bones in (A) posterodorsal view with (B) labeled drawing. (C) Depression housing cranial nerves. Braincase in (D) posterior view with (D) labeled drawing. Abbreviations: bo, basioccipital; bs, basisphenoid; eo, exoccipital; fm, foramen magnum; oc, occipital condyle; op, opisthotic; pop; paroccipital process; r, ridge; so, supraoccipital; vcd, foramen vena capitis dorsalis; X, X(I) XI(I) foramina for cranial nerves; ?, unknown bone. Striated area indicates damage. Scale bar presents 50 mm. Photos by Xiao-Chun Wu.

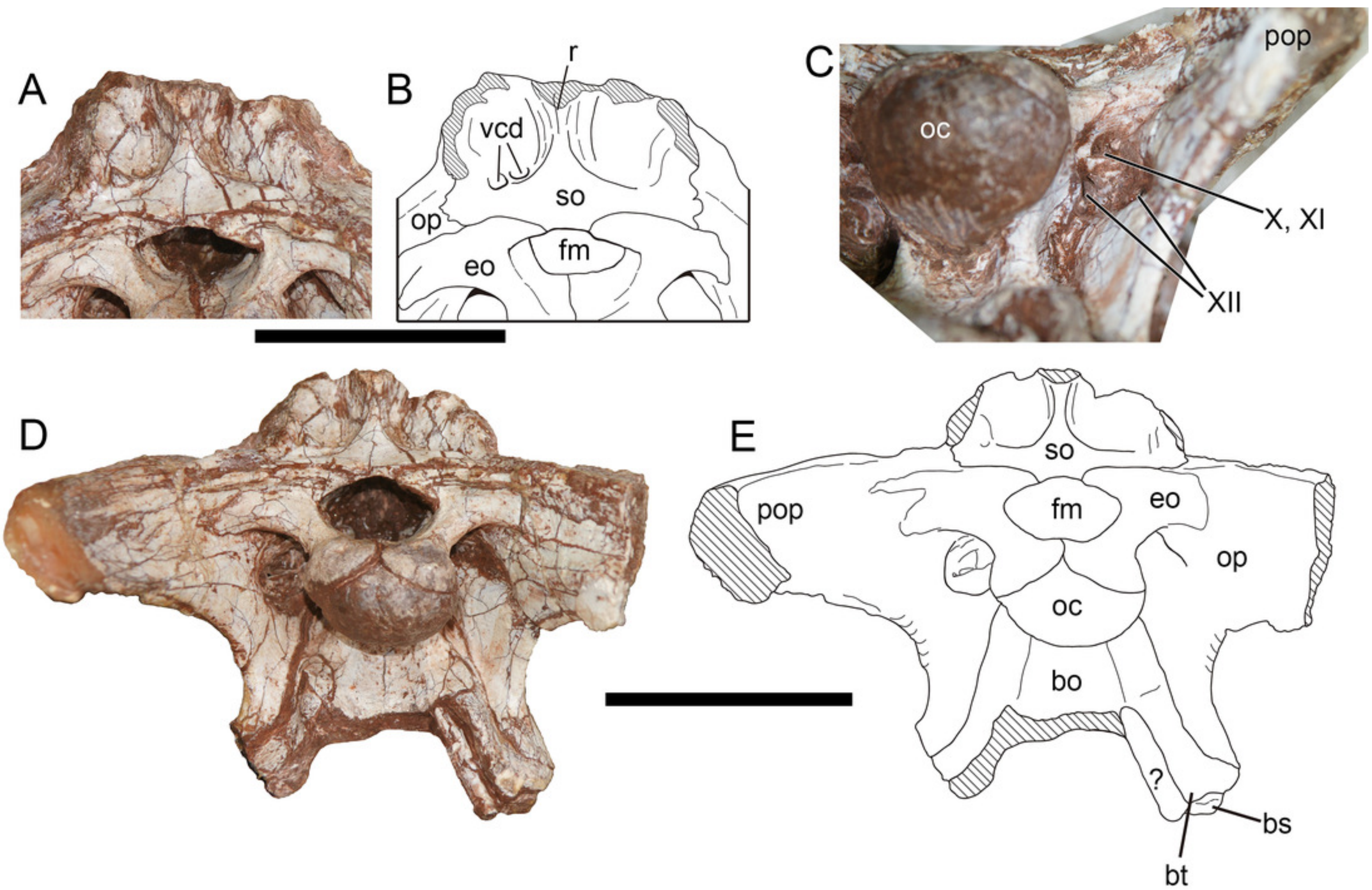

Figure 9

Braincase of *Yuanmouraptor jinshajiangensis* gen. et sp. nov. (LFGT-ZLJ0015).

Braincase in (A) lateroposterior view with (B) labeled drawing and in (C) laterodorsal view with (D) labeled drawing. Abbreviations: bo, basioccipital; bs, basisphenoid; bt, basal tuber; cfp, cultriform process; cp, crista prootica; fo, fenestra ovalis; lsp, laterosphenonid; oc, occipital condyle; op, opisthotic; pa, parietal; po, postorbital; pop, paroccipital process; pp, prootic pendant; pr, prootic; vcd, foramen vena capitis dorsalis; VI(I) cranial nerve VII (facial nerve); so, supraoccipital. Straited area inidcates damage and grey area indicates matrix. Scale bar presents 50 mm. Photos by Xiao-Chun Wu.

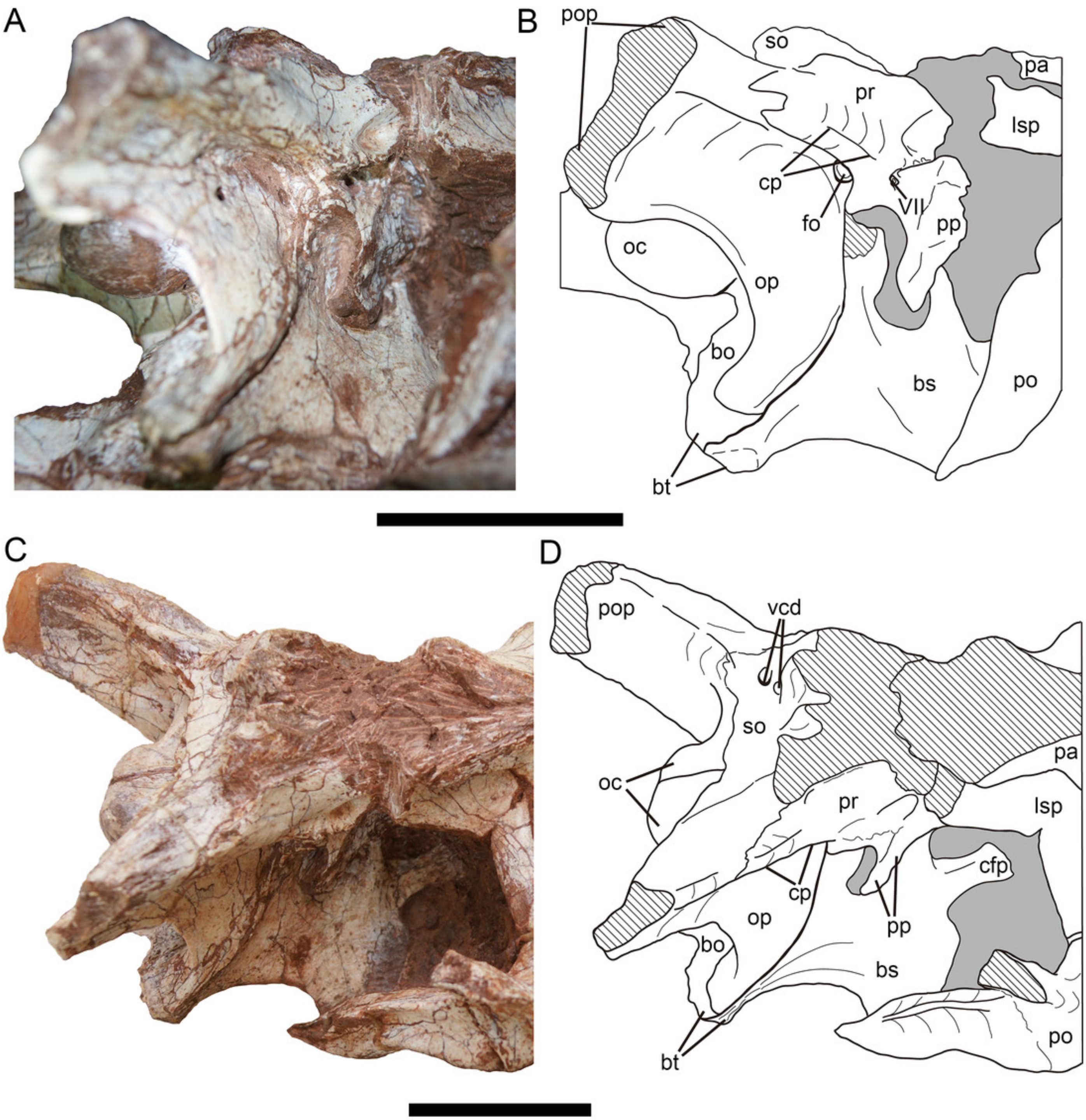
A
B
pop
so
pa
pr
lsp
cp
VII
fo
pp
oc
op
bo
bs
po
bt
C
D
pop
vcd
so
pa
oc
pr
lsp
cfp
cp
pp
op
bo
bs
bt
po

Figure 10

Mandibular elements of *Yuanmouraptor jinshajiangensis* gen. et sp. nov. (LFGT-ZLJ0015).

Left dentary in (A) lateral view with (B) labeled drawing. Left posterior part of mandible in (C) lateral view with (D) labeled drawing. Right posterior part of mandible in (E) medial view with (F) labeled drawing. Abbreviations: af, adductor fossa; an, angular; ar, articular; ct, foramen of condra typamni; d4-14, dentary teeth 4-14; emf, external mandibular fenestra; g, groove; hp, hook like process of surangular; imf, internal mandibular fenestra; lg, lateral glenoid; mame, attachment of M. adductor mandibulae externus; nf, neurovascular foramina. par, prearticular; psf, posterior surangular foramen; retp, retroarticular process; sa, surangular; sp, splenial; sr, surangular ridge. Striated area indicates damage. Scale bar presents 50 mm. Photos by Xiao-Chun Wu and Yi Zou.

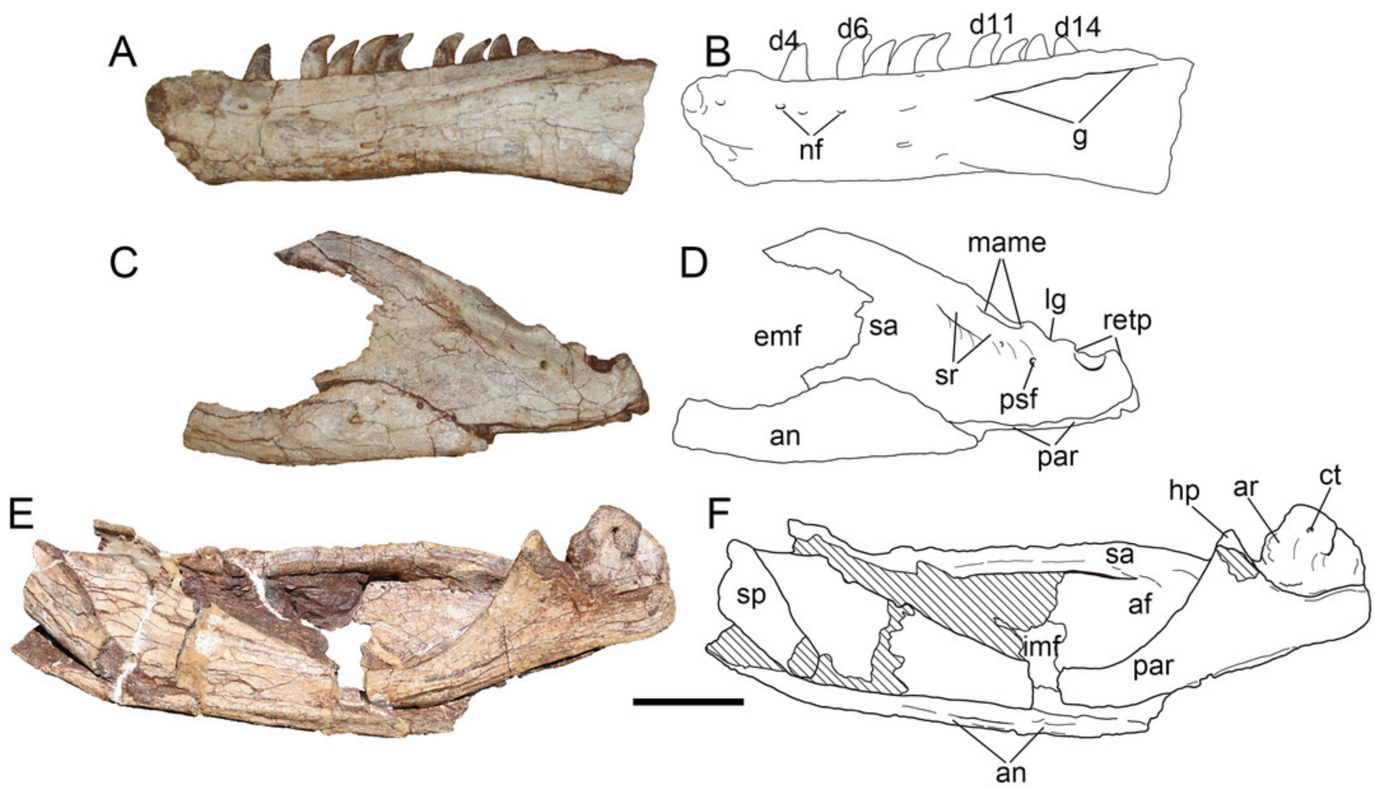

Figure 11

Mandibular joint of *Yuanmouraptor jinshajiangensis* gen. et sp. nov. (LFGT-ZLJ0015).

Right mandibular joint in (A) lateral view with (B) labeled drawing and in (C) dorsal view with (D) labeled drawing. Abbreviations: ar, articular; ct, foramen of condra typamni; hp, hook like process of surangular; lg, lateral glenoid; mame, attachment of M. adductor mandibulae externus; mg, medial glenoid; par, prearticular; psf, posterior surangular foramen; r, ridge; retp, retroarticular process; sa, surangular; sr, surangular ridge. Scale bar presents 50 mm. Photos by Xiao-Chun Wu and Yi Zou.

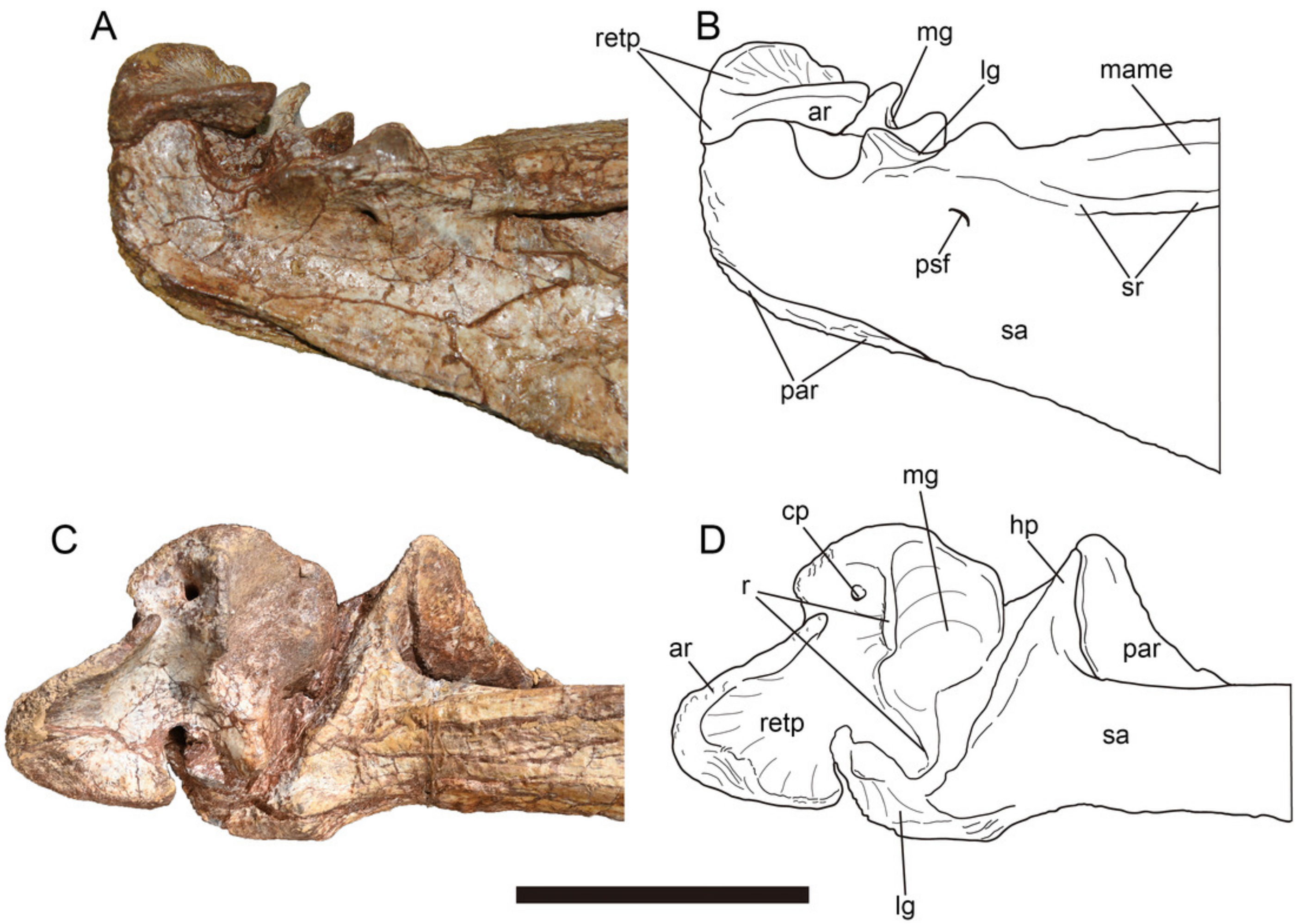

Figure 12

Atlas-axis complex of *Yuanmouraptor jinshajiangensis* gen. et sp. nov. (LFGT-ZLJ0115).

Atlas-axis complex in ((A)), dorsal, (B) ventral, (C) anterior, (D) posterior, (E) right lateral and (F) left lateral views. Abbreviations: ati, atlantal intercentrum; axi, axial intercentrum; dp, diapophysis; ep, epipophysis; na, neurapophysis; nc, neural canal; od, odontoid; poz, postzygopophysis; pp, parapophysis; re, rounded eminence; spol, spinopostzygipophyseal lamina; tpol, intrapostzygopophyseal lamina. All names of the bony laminae follow terminologies in *Wilson (1999)*. Scale bar presents 50 mm. Photos by Xiao-Chun Wu.

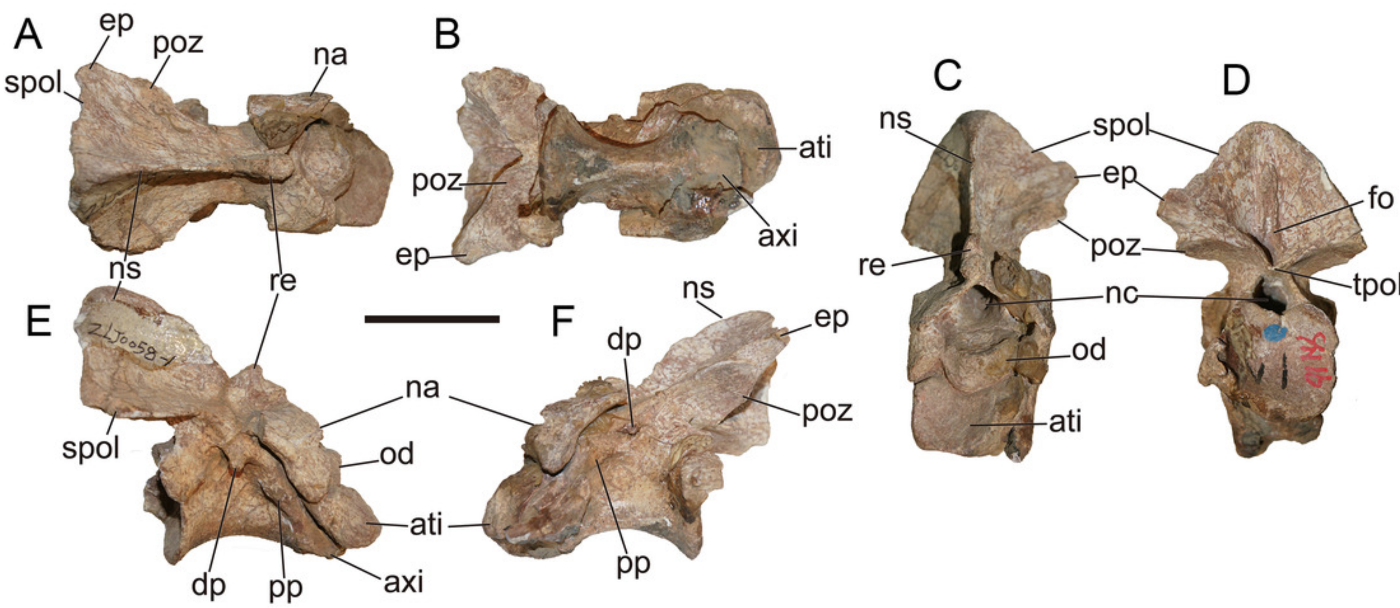

Figure 13

Postaxial vertebrae of *Yuanmouraptor jinshajiangensis* gen. et sp. nov. (LFGT-ZLJ0115).

Postaxial vertebrae in lateral view. (A) Cervical 3; (B) Cervical 4; (C) Cervical 5; (D) Cervical 6; (E) Cervical 7; (F) Cervical; (G) Cervical 9; (H) Cervical 10; (I) Dorsal 1. Abbreviations: acdl, anterior centrodiapophyseal lamina; cpol, centropostzygopophyseal lamina; cprl, centroprezygopophyseal lamina; dp, diapophysis; ep, epipophysis; ns, neural spine; pcdl, posterior centrodiapophyseal lamina; pl, pleurocoel; podl, postzygodiapophyseal lamina; poz, postzygopophysis; pp, parapophysis; prdl, prezygodiapophyseal lamina; prz, prezygopophysis; spol, spinopostzygopophyseal lamina; ri, distinct rim on the anterior articular surface; sprl, spinoprezygodiapophyseal lamina; vk, ventral keel. All names of the bony laminae follow terminologies in *Wilson (1999)* . Scale bar presents 50 mm. Photos by Xiao-Chun Wu.

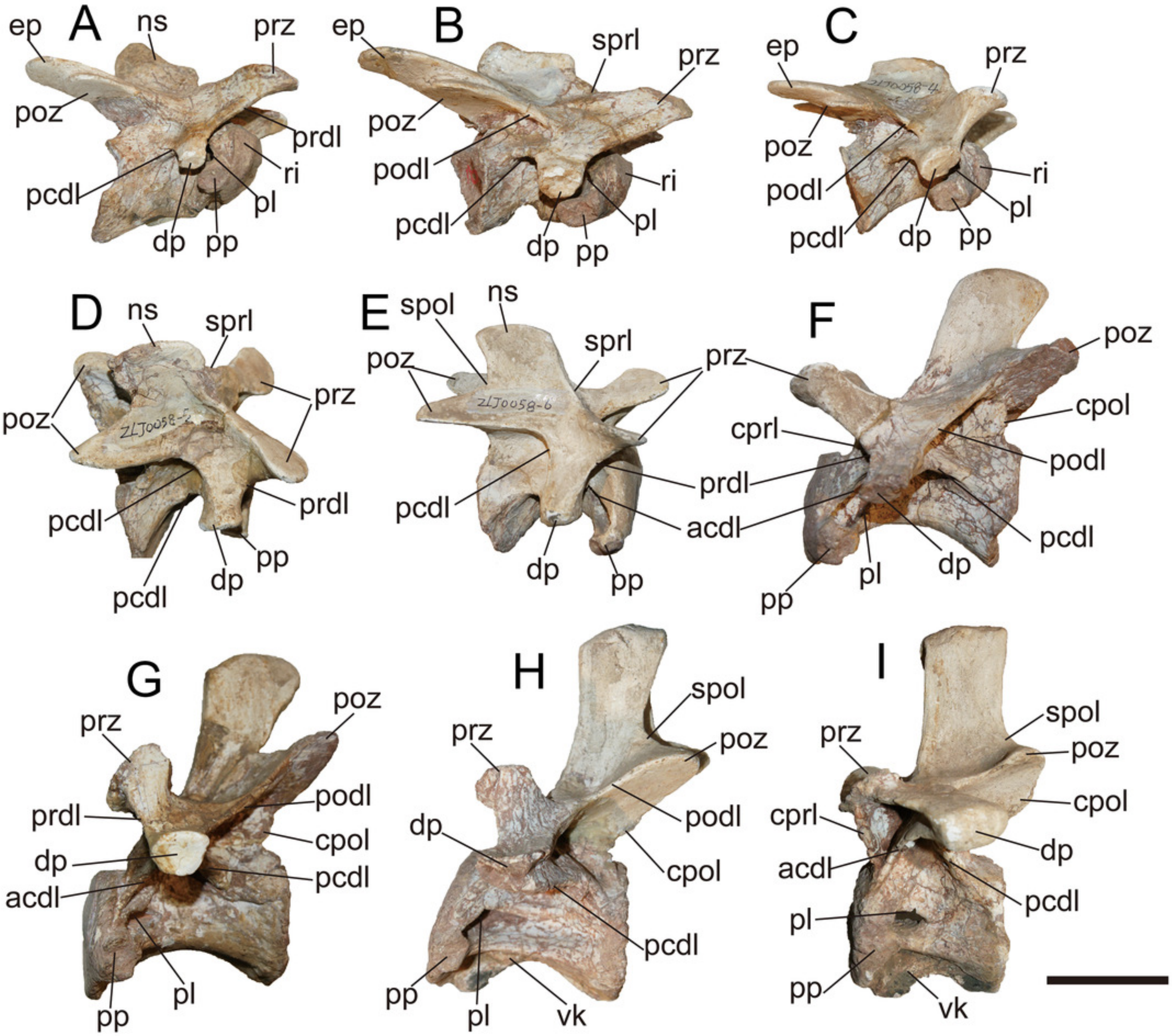
A
ep
ns
prz
poz
prdl
ri
pcdl
pl
dp
pp
B
ep
sprl
prz
poz
podl
ri
pcdl
pl
dp
pp
C
ep
prz
poz
podl
ri
pcdl
pl
dp
pp
D
ns
sprl
poz
prz
ZLJ0058-5
pcdl
prdl
pp
dp
pcdl
E
spol
ns
sprl
poz
prz
ZLJ0058-6
pcdl
prdl
acdl
dp
pp
F
prz
poz
cprl
cpol
podl
prdl
acdl
pcdl
pp
pl
dp
G
prz
poz
podl
prdl
cpol
dp
pcdl
acdl
pl
pp
H
spol
prz
poz
dp
podl
cpol
pcdl
pp
pl
vk
I
spol
prz
poz
cprl
cpol
acdl
dp
pcdl
pl
pp
vk

Figure 14

Postaxial vertebrae of *Yuanmouraptor jinshajiangensis* gen. et sp. nov. (LFGT-ZLJ0115).

Cervical 3 in (A) anterior, (B) posterior, (C) ventral, (D) dorsal views. Cervical 5 in (E) ventral, (F) posterior views. Cervical 9 in (G) anterior, (H) posterior, (I) dorsal views. Abbreviations: cpol, centropostzygopophyseal lamina; cprl, centroprezygopophyseal lamina; ep, epipophysis; nc, neural canal; ns, neural spine; pl, pleurocoel; podl, postzygodiapophyseal lamina; poz, postzygopophysis; prz, prezygodiapophyseal lamina; ri, distinct rim on the anterior articular surface; tpol, intrapostzygopophyseal lamina; tprl, itraprezygopophyseal lamina; spol, spinopostzygopophyseal lamina. All names of the bony laminae follow terminologies in *Wilson (1999)*. Scale bar presents 50 mm. Photos by Xiao-Chun Wu.

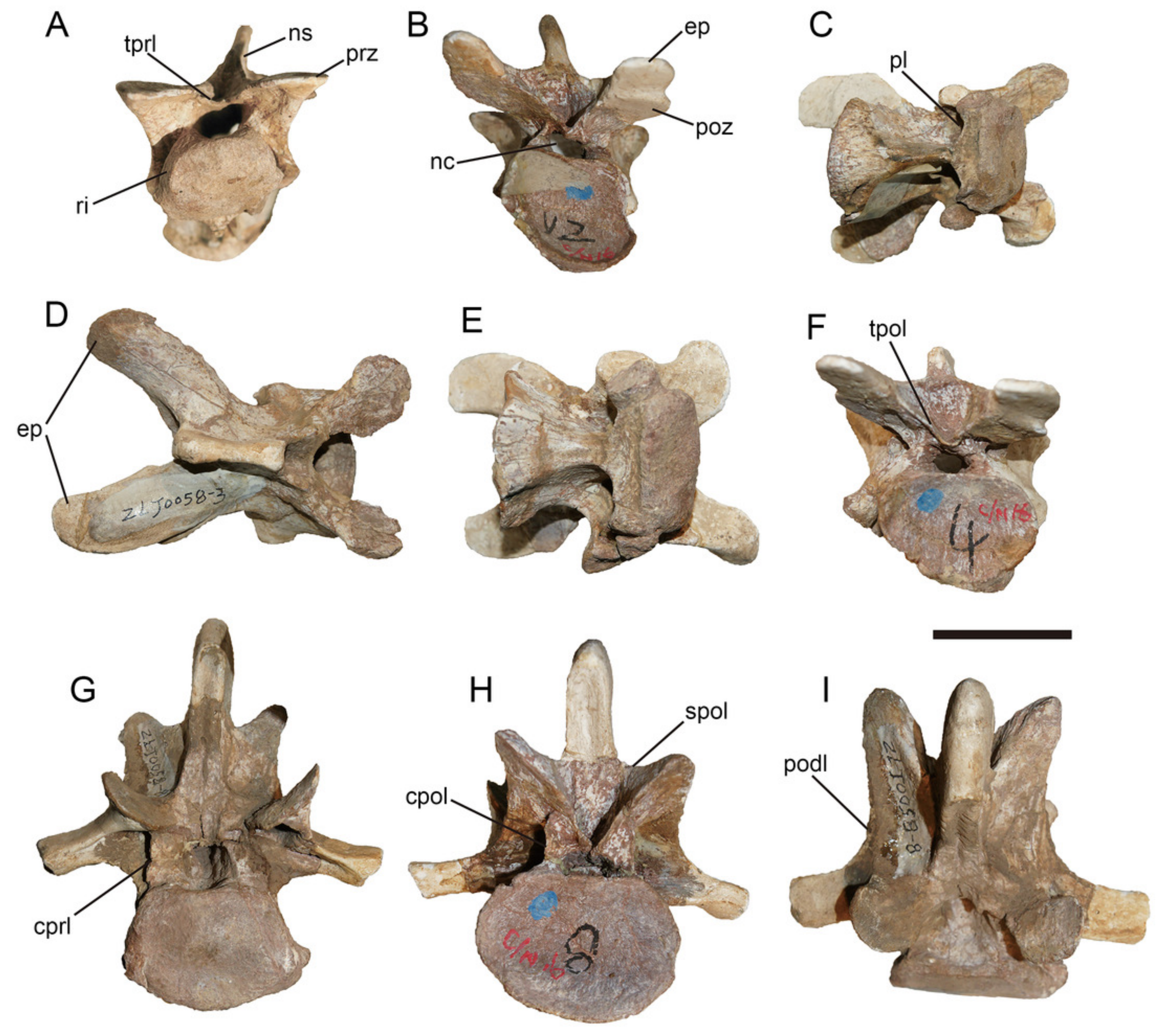
A
tprl
ns
prz
ri
B
ep
poz
nc
C
pl
D
ep
E
F
tpol
G
cprl
H
spol
cpol
I
podl

Figure 15

Result of phylogenetic analysis

Time-Calibrated strict consensus tree showing the phylogenetic position of *Yuanmouraptor* with the latest geological time scale.